Numerical Solutions of the One-Dimensional Saturated-Unsaturated Flow Equation

M. Th. van Genuchten

November 1978

Research Report 78-WR-09

Water Resources Program
Department of Civil Engineering
Princeton University
Princeton, NJ

Numerical Solutions of the One-Dimensional Saturated-Unsaturated Flow Equation

by

*M. Th. van Genuchten**

Water Resources Program
Department of Civil Engineering
Princeton University
Princeton, New Jersey 08540

*Present address: George E. Brown Jr., Salinity Laboratory
450 West Big Springs Road, Riverside, CA 92507

78-WR-09

November 1978

ABSTRACT

Several finite difference and Galerkin-type finite element solutions of the one-dimensional saturated-unsaturated flow equation are presented. Both zero-order continuous linear and first-order continuous Hermitian (cubic) finite element formulations are considered. It is concluded that the linear (LFE) and Hermitian finite element (HFE) schemes may cause some oscillations near the toe of the moisture front when infiltration in dry soil is simulated. This is especially the case when a first type (constant pressure) boundary condition is imposed on the system. No such oscillations were observed with a finite difference scheme (FD). By applying mass-lumping to the time derivative in the linear finite element formulation (MFE), one can also effectively remove these undesired oscillations. The HFE-scheme always generated the most accurate solution of the moisture front, but at the expense of more computation time. The FD- and MFE-schemes are preferred when infiltration in extremely dry soil needs to be simulated. The HFE-scheme becomes very competitive with the various zero-order continuous schemes for somewhat less extreme cases, both with respect to accuracy and computational efficiency.

The listing of a generalized Hermitian finite element computer model (UNSAT1) is given in an appendix of this report. The model may be used to simulate moisture movement in a one-dimensional, saturated-unsaturated and non-homogeneous soil profile. Both abrupt layering and smoothly changing profile properties are considered in the model.

ACKNOWLEDGEMENTS

The author is indebted to Professor George F. Pinder for reviewing an earlier draft of this report. This work was supported in part by funds obtained from the Solid and Hazardous Waste Research Division, U. S. Environmental Protection Agency, Municipal Research Laboratory, Cincinnati, Ohio (EPA Grant No. R803827-01).

TABLE OF CONTENTS

NOTATION

a	Parameter defined by Eq. (35a).
a_j	Entries in unknown coefficient matrix $\{X\}$.
$[A]$	Coefficient matrix in global matrix equation.
b	Parameter defined by Eq. (35b).
$[B]$	Coefficient matrix of time derivative in global matrix equation.
c	Parameter defined by Eq. (35c).
C, C^*	Specific soil moisture capacity (L^{-1}).
$\hat{C}_i$	Value of C at i-th node (L^{-1}).
C	Spatial distribution of C over an arbitrary element (L^{-1}).
f	Parameter defined by Eq. (35d).
$\{F\}$	Right-hand side vector of global matrix equation.
h	Pressure head (L).
h_i	Initial pressure head (L).
h_ℓ	Pressure head at $x = \ell$ (L).
h_o	Pressure head at $x = 0$ (L).
$\hat{h}$	Finite element approximation of pressure head (L).
h_i^k	Estimated pressure head at i-th node and k-th iteration (L).
h_i^t	Value of pressure head at i-th node and time t (L).
H_i	Nodal values of pressure head (L).
k	Number of numerical integration points.

NOTATION (continued):

K	Hydraulic conductivity (LT^{-1}).
K_A, K_B	Hydraulic conductivity of soil types A and B (LT^{-1}).
K_{cl}, K_{ls}	Hydraulic conductivity of clay loam and loamy sand (LT^{-1}).
K_s	Saturated hydraulic conductivity (LT^{-1}).
$\hat{K}$	Hydraulic conductivity distribution over an arbitrary element (LT^{-1}).
ℓ	Depth of soil profile (L).
L	Operator on h as defined by Eq. (1).
m	Parameter defined by Eq. (39).
n	Parameter in Eq. (45); also used for the number of equations in the finite element solution.
$[P]$	Global coefficient matrix for new time level.
q	Volumetric flux (LT^{-1}).
q_ℓ	Volumetric flux at $x = \ell$ (LT^{-1}).
q_o	Volumetric flux at $x = 0$ (LT^{-1}).
$\hat{q}$	Distribution of q over an arbitrary element (LT^{-1}).
$[Q]$	Global coefficient matrix for old time level.
S_s	Specific storage coefficient (L^{-1}).
S_w	Degree of fluid saturation.
t	Time (T).
x	Vertical distance (L).

NOTATION (continued):

x_i	x-coordinate of i-th node (L).
$\{X\}$	Vector of unknown coefficients.
w_i	Weighting factor for i-th numerical integration point.
Δt	Time increment (T).
Δt_n	New time increment (T).
Δt_o	Old time increment (T).
Δx	Nodal distance (L).
ϵ	Porosity.
θ	Volumetric moisture content.
θ_i	Initial moisture content.
θ_ℓ	Moisture content at $x = \ell$.
θ_o	Moisture content at $x = 0$.
θ_r	Residual moisture content.
θ_s	Saturated moisture content.
$\hat{\theta}$	Moisture content distribution over an arbitrary element.
Θ	Dimensionless moisture content.
μ_1	Absolute convergence criterion (L).
μ_2	Relative convergence criterion.
ξ	Local coordinate.
ξ_0	Parameter appearing in definition of basis functions.

NOTATION (continued):

ξ_i	ξ-coordinate of i-th integration point.
ϕ_j	General basis functions.
ϕ_j^0	Linear basis functions.
ϕ_{0j}^0, ϕ_{1j}^1	Hermitian basis functions.
ω	Weighting coefficient.

LIST OF FIGURES

LIST OF FIGURES (continued):

LIST OF TABLES

1. INTRODUCTION

A quantitative understanding of moisture flow in unsaturated or partly saturated soils is of considerable importance for scientists working in irrigation and drainage, soil science, groundwater hydrology, and water resources. Much literature exists today that deals with the mathematical solution of the governing flow equation, using both analytical and numerical techniques. In the analytical approach the governing equations, the analytic representation of the soil-hydraulic properties, and the initial and boundary conditions imposed on the simulated system are suitably simplified or approximated such that exact or "quasi-analytical" solutions can be derived. Some typical examples of this approach are given in the list of references (1-11). An important advantage of the analytical approach, even if based upon simplifying assumptions, is that its solutions often more clearly demonstrate the fundamental nature of the flow processes and its dependence upon certain flow and soil parameters. In addition, analytical solutions are invaluable tools for verifying the accuracy of numerical solutions.

Important advantages of numerical solutions, on the other hand, are that actual soil properties and less restrictive initial and boundary conditions can be included in the solution procedure. Many studies can be cited where this tool has been used to solve the one-dimensional unsaturated flow equation (see references 12-43). In many others numerical techniques have been used for solution of the two-dimensional flow equation, as well as for solution of the combined water and solute transport equations, both in one and two dimensions.

Most of the earlier studies on unsaturated flow have used finite difference techniques for solution of the flow equation. In this approach, one approximates the partial derivatives in the governing partial differential equation by appropriate difference quotients. A close examination of some of the cited references shows that in this way, and depending upon the type and accuracy of the approximation, several different schemes can be developed. In a recent review article, Haverkamp *et al.*[42] compared six of the most frequently used schemes and found that considerable differences in computational efficiency existed between the different formulations. Depending upon the infiltration experiment considered, the less efficient schemes consumed up to ten times more computer time than the more efficient ones.

Lately Galerkin and equivalent finite element techniques have been used also to solve the unsaturated flow equation. In this approach the dependent variables, such as pressure head or moisture content, are approximated by a series of basis (or shape) functions and associated, time-dependent coefficients. The approximating series are then substituted into the governing equations and the resulting errors ("residuals") minimized through the use of weighted-residual theorems. The integral equations derived in this way are evaluated using the finite-element method of discretization, resulting in a set of (quasi-) linear equations which can be solved by using appropriate matrix equation solvers. Several finite element schemes can be developed, depending upon the type of basis functions used (linear, quadratic, zero- or first-order continuous cubic basis functions), and the method by which the integrals in the numerical formulation are evaluated (closed-form or numerical

evaluation; number and type of integration points).

In this report a finite element solution of the one-dimensional saturated-unsaturated flow equation is developed which uses first-order continuous cubic (Hermitian) polynomials as its basis functions. A fully documented listing of the program (UNSAT1) is given at the end of this report. Results obtained with the Hermitian finite element scheme are compared with those based on ("standard") finite differences and linear finite elements. An example problem, furthermore, demonstrates how the Hermitian finite element code can be used to study moisture flow in non-homogeneous and layered field soils.

2. THEORETICAL DEVELOPMENT

2.1. Governing equations

The partial differential equation governing the one-dimensional vertical flow of moisture in a saturated-unsaturated medium is given by

$$L(h) \equiv \frac{\partial}{\partial x}\left(K \frac{\partial h}{\partial x} - K\right) - \left(\frac{\theta}{\varepsilon} S_s + C^*\right) \frac{\partial h}{\partial t} = 0 \qquad (1)$$

where

- K is the hydraulic conductivity (LT^{-1}),
- h is the pressure head (L),
- θ is the volumetric moisture content,
- S_s is the specific storage coefficient (L^{-1}),
- ε is the porosity,
- C^* is the specific soil moisture capacity (L^{-1}): $C^* = \varepsilon \frac{\partial S_w}{\partial h}$,
- S_w is the degree of fluid saturation,
- x is the vertical spatial coordinate (positive down) (L), and
- t is time (T).

Equation (1) contains several assumptions. For example, it is assumed that the air phase dynamics plays an insignificant role in the unsaturated zone, and that as a consequence a single equation can be used to describe saturated-unsaturated flow. The fluid density, furthermore, is assumed to be concentration and temperature independent, while spatial variations in the fluid density are assumed to be insignifi-

cantly small. Equation (1) is highly non-linear, especially in the unsaturated zone, due to the dependency of the hydraulic conductivity, K, the specific moisture capacity, C^*, and the soil moisture content, θ, on the pressure head, h. This study does not consider hysteresis in any of these functional relationships. The term containing S_s in (1) is generally insignificantly small compared to C^* when only an unsaturated zone is considered. The coefficient of the time derivative may then be approximated by

$$\frac{\theta}{\varepsilon} S_s + C^* \simeq \varepsilon \frac{\partial S_w}{\partial h} \tag{2}$$

$$\simeq \frac{d\theta}{dh} .$$

Denoting the slope of the moisture content - pressure head curve $\left(\frac{d\theta}{dh}\right)$ by C, equation (1) becomes

$$L(h) \equiv \frac{\partial}{\partial x} \left(K \frac{\partial h}{\partial x} - K\right) - C \frac{\partial h}{\partial t} = 0 \tag{3}$$

The initial condition imposed on the system is

$$h(x,0) = h_i(x) . \tag{4}$$

Any of the two following boundary conditions may be imposed at the soil surface (x=0):

$$h(0,t) = h_o(t) \tag{5a}$$

$$\left(-K \frac{\partial h}{\partial x} + K\right)\Big|_{x=0} = q_o(t) \tag{5b}$$

where $q_o(t)$ is the actual (net) flux at the soil surface (i.e., precipitation + irrigation - evaporation). Boundary condition (5b) can be rearranged in terms of the pressure gradient:

$$\left.\frac{\partial h}{\partial x}\right|_{x=0} = 1 - q_o(t)/K. \tag{5c}$$

Essentially the same conditions may be applied to the lower boundary of the soil profile ($x=\ell$), i.e.

$$h(\ell,t) = h_\ell(t) \tag{6a}$$

$$\left(-K \frac{\partial h}{\partial x} + K\right)\Big|_{x=\ell} = q_\ell(t) \tag{6b}$$

where $q_\ell(t)$ is the imposed drainage flux. If boundary condition (6b) applies, the pressure gradient at $x=\ell$ becomes

$$\left.\frac{\partial h}{\partial x}\right|_{x=\ell} = 1 - q_\ell(t)/K. \tag{6c}$$

Finally, when a free draining soil profile is considered, q_ℓ equals K at $x=\ell$, and (6c) reduces to

$$\left.\frac{\partial h}{\partial x}\right|_{x=\ell} = 0. \tag{6d}$$

2.2. *Galerkin approximation*

Because details of the Galerkin finite element method have been discussed at length elsewhere[44,45], only its basic concepts will be reviewed here. In the finite element approach the dependent variable, h, is approximated by a finite series of the form

$$h(x,t) \simeq \hat{h}(x,t) = \sum_{j=1}^{n} \phi_j(x)\, a_j(t) \tag{7}$$

where the $\phi_j(x)$ are the selected basis functions and the $a_j(t)$ the associated, unknown, time-dependent coefficients which represent solutions of (3) at specified points ("nodes") within the domain. The approximate solution $\hat{h}(x,t)$ converges to the correct solution $h(x,t)$ when n approaches infinity. Because only a finite number of basis functions are used in expansion (7), the residual $L(\hat{h})$ arising when (7) is substituted into (3) will generally not be zero. This residual, however, may be minimized by requiring that $L(\hat{h})$ be orthogonal to a set of mutually independent weighting functions. In the Galerkin method these weighting functions are chosen to be identical to the basis functions $\phi_j(x)$ in (7). From the definition of orthogonal functions, this can be expressed as

$$\int_0^{\ell} L(\hat{h})\, \phi_i(x)\, dx = 0 \qquad (i=1,\ldots,n) \tag{8}$$

or, with Eq. (3):

$$\int_0^{\ell} \left[\frac{\partial}{\partial x}\left(K \frac{\partial \hat{h}}{\partial x} - K\right) - C \frac{\partial \hat{h}}{\partial t}\right] \phi_i = 0, \tag{9}$$

Integration by parts of the spatial derivations gives

$$\int_0^{\ell} \left(K \frac{\partial \hat{h}}{\partial x} - K\right) \frac{d\phi_i}{dx}\, dx + \int_0^{\ell} C \frac{\partial \hat{h}}{\partial t}\, \phi_i\, dx = -\hat{q}\, \phi_i \Big|_0^{\ell} \tag{10}$$

where

$$\hat{q} = -\left(K \frac{\partial \hat{h}}{\partial x} - K\right). \tag{11}$$

When the series expansion (7) is substituted into (10) the following matrix equation results

$$[A]\,\{X\} + [B]\,\left\{\frac{dX}{dt}\right\} = \{F\} \tag{12}$$

where

$$[A_{ij}] = \int_0^{\ell} K \frac{d\phi_j}{dx} \frac{d\phi_i}{dx}\, dx \tag{13a}$$

$$[B_{ij}] = \int_0^{\ell} C\, \phi_j\, \phi_i\, dx \tag{13b}$$

$$\{X_i\} = a_i \tag{13c}$$

$$\{F_i\} = -\hat{q}\, \phi_i \Big|_0^{\ell} + \int_0^{\ell} K \frac{d\phi_i}{dx}\, dx. \tag{13d}$$

The unknown coefficients a_i are obtained by first evaluating the integrals in (13) and subsequently solving (12). The approximate solution $\hat{h}(x,t)$ follows then directly by substitution of these coefficients into (7). Equation (12) defines a set of n ordinary differential equations with

non-linear coefficients. A finite difference scheme may be introduced to approximate the time derivative in the matrix equation. Define for that purpose the following approximations

$$\left\{\frac{dX}{dt}\right\}^{t+\frac{1}{2}\Delta t} \simeq \frac{\{X\}^{t+\Delta t} - \{X\}^{t}}{\Delta t} \tag{14a}$$

$$\{X\}^{t+\frac{1}{2}\Delta t} = \omega \{X\}^{t+\Delta t} + (1-\omega) \{X\}^{t} \tag{14b}$$

where Δt is the time step and ω a temporal weighting coefficient ($0 \leq \omega \leq 1$). By defining matrix Eq. (12) at the half-time level ($t+\frac{1}{2}\Delta t$), and introducing approximations (14a) and (14b), the following set of n algebraic equations results

$$[P]^{t+\frac{1}{2}\Delta t}\{X\}^{t+\Delta t} = [Q]^{t+\frac{1}{2}\Delta t} \{X\}^{t} + \{F\}^{t+\frac{1}{2}\Delta t} \tag{15}$$

where

$$[P] = \omega[A] + \frac{1}{\Delta t} [B] \tag{16a}$$

$$[Q] = (\omega-1) [A] + \frac{1}{\Delta t} [B]. \tag{16b}$$

When ω=1 essentially an implicit in time (backward) finite difference scheme results, even though the various coefficient matrices still are evaluated at the half-time level ($t+\frac{1}{2}\Delta t$). By evaluating the coefficients at the half-time level an under-relaxation technique is, in effect, employed, leading to less oscillations and generally a much faster convergence. Such implicit schemes were previously used by Segol[46]

and Frind *et al.*[47] When, on the other hand, $\omega=\frac{1}{2}$, a time-centered, Crank-Nicolson type algorithm is obtained from (15) (Neuman[28]).

To be able to solve (15), one needs estimates of the coefficients K and C in (13) at the half-time level $(t+\frac{1}{2}\Delta t)$. Because these coefficients depend on the pressure head, it is in turn necessary to have an estimate of the pressure head distribution, $\hat{h}$, at the half-time level. For each new time step this distribution is obtained through linear interpolation from the old distributions as follows:

$$\hat{h}^{t+\frac{1}{2}\Delta t} = \hat{h}^{t} + \frac{\Delta t_n}{2\Delta t_o} (\hat{h}^{t} - \hat{h}^{t-\Delta t}) \tag{17}$$

where Δt_o and Δt_n are the old and new time increments, respectively. Because (15) is non-linear, the initial estimate must be improved by means of an iterative process. During each iteration the most recent distribution of $\hat{h}^{t+\Delta t}$, obtained by solving (15) and making use of (7), is used to obtain a new estimate for the half-time level:

$$\hat{h}^{t+\frac{1}{2}\Delta t} = \frac{1}{2} (\hat{h}^{t+\Delta t} + \hat{h}^{t}). \tag{18}$$

The iterative process continues until a satisfactory degree of convergence is obtained. The criterion of convergence, in its most general form, is given by

$$\left|\hat{h}_i^{k+1} - \hat{h}_i^{k}\right| \leq \mu_1 + \mu_2 \left|\hat{h}_i^{k+1}\right| \tag{19}$$

where k represents the iteration number, and where $\hat{h}_i = \hat{h}(x_i)$, to be evaluated at the new time level. If μ_1 equals zero, the iteration

process stops when the relative change in $\hat{h}_i$ between two successive iterations becomes less than μ_2. If, on the other hand, μ_2 equals zero, the iterative process stops when the absolute change in $\hat{h}_i$ between two successive iterations becomes less than the given value of μ_1.

2.3. *Basis functions*

To facilitate evaluation of the integrals appearing in (13), the soil profile may be subdivided into an assemblage of subdomains or "elements". The basis functions $\phi_j(x)$ are then used to spatially approximate the unknown function over each element separately. Several sets of basis functions are available for this purpose, such as the zero-order continuous linear, quadratic or cubic basis functions. These functions characteristically attain a unit value at one nodal point of the element, and a zero value at the remaining nodes, while they are identical to zero outside the element considered. From this definition it follows immediately that the integrals in (13) only need to be evaluated once over each single element, and that the unknown coefficients $a_j(t)$ now coincide with the values of the dependent variable, h, at the node for which the basis function was defined. For a linear, one-dimensional element, for example, Eq. (7) reduces to

$$\hat{h}(x,t) = \phi_1^0(x)\ H_1(t) + \phi_2^0(x)\ H_2(t) \tag{20}$$

where $H_1(t)$ and $H_2(t)$ represent the unknown pressure head values at the two corner nodes of the element. The basis functions can be written in terms of a local (ξ) coordinate system, as follows[48]

$$\phi_j^0 = \frac{1}{2}(1+\xi_0\xi) \qquad (\xi_0 = \pm 1). \tag{21}$$

The local coordinate, ξ, is defined in terms of the global coordinate system, x, as

$$\xi = \frac{2(x-x_1)}{\Delta x} - 1 \qquad (x_1 < x < x_2) \tag{22}$$

where $\Delta x = (x_2-x_1)$ represents the nodal distance of the element.

A special class of basis functions is based on Hermitian polynomials. If these are used, one not only solves for the values of the function itself, but also for the values of the spatial derivatives. For example, the approximating function $\hat{h}$, when used in conjunction with the one-dimensional first-order continuous cubic (Hermitian) basis functions, becomes

$$\hat{h}(x,t) = \sum_{j=1}^{2} \left(\phi_{0j}^{1}(x)\, H_j(t) + \phi_{1j}^{1}(x)\, \frac{dH_j}{dx}(t) \right) \tag{23}$$

with the Hermitian basis functions, in terms of the ξ coordinate, given by[49]

$$\phi_{0j}^{1} = -\frac{1}{4}(\xi+\xi_0)^2(\xi\xi_0-2) \qquad (\xi_0=\pm 1) \tag{24a}$$

$$\phi_{1j}^{1} = \frac{\Delta x}{8}\,\xi_0(\xi+\xi_0)^2(\xi\xi_0-1) \qquad (\xi_0=\pm 1) \tag{24b}$$

Figure 1 gives a graphical representation of the four basis functions defined by (24).

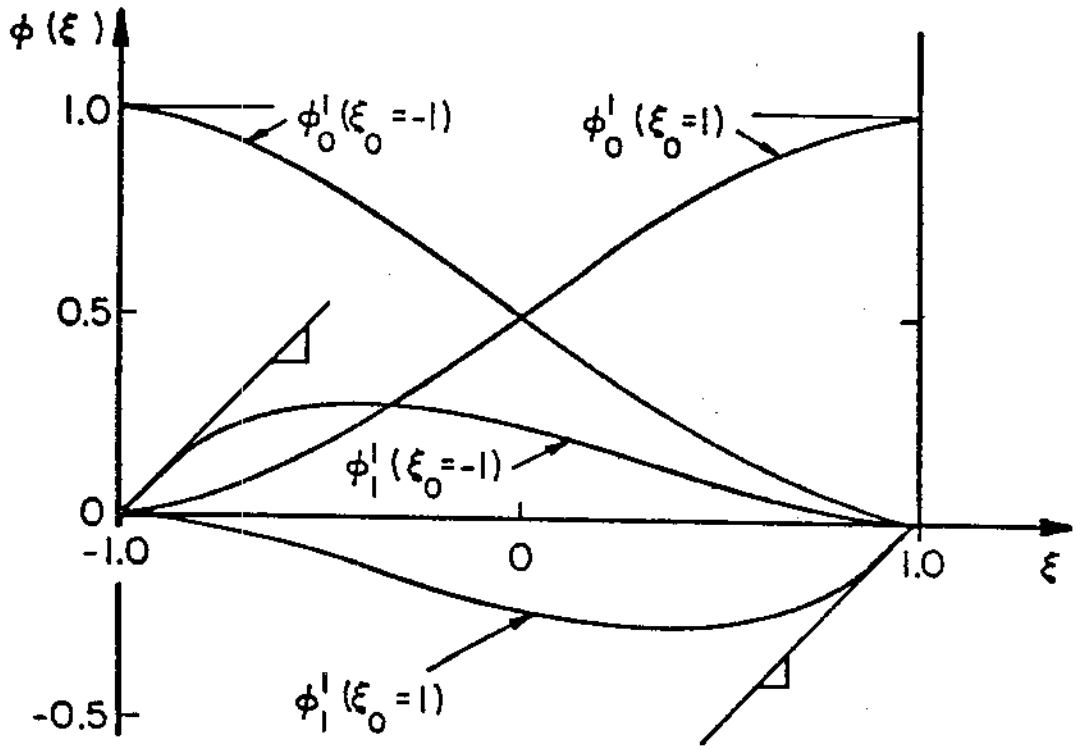

Fig. 1. First-order continuous Hermitian basis functions[50].

2.4. *Numerical implementation*

At least two approaches are possible for evaluating the integrals appearing in Eq. (13). One possible approach is to expand the coefficients K and C over each element in terms of the basis functions and the values of K and C at the nodes, analogous to Eq. (20) and (23). The advantages of this approach is that the integrations then need to be carried out only once. For a linear element one hence has

$$\hat{K}(\xi) = \sum_{k=1}^{2} K_k \, \phi_k^0(\xi) \tag{25a}$$

$$\hat{C}(\xi) = \sum_{k=1}^{2} C_k \, \phi_k^0(\xi) \tag{25b}$$

where K_k and C_k represent the nodal values of the two coefficients. By substituting Eq. (25a) and (25b) into (13), and using (22), the different coefficient matrices become

$$[A] = \frac{1}{2\Delta x} \begin{bmatrix} K_1+K_2 & -K_1-K_2 & & & 0 \\ -K_1-K_2 & K_1+2K_2+K_3 & -K_2-K_3 & & \\ & \ddots & \ddots & \ddots & \\ & & -K_{n-2}-K_{n-1} & K_{n-2}+2K_{n-1}+K_n & -K_{n-1}-K_n \\ 0 & & & -K_{n-1}-K_n & K_{n-1}+K_n \end{bmatrix} \tag{26a}$$

$$[B] = \frac{\Delta x}{12} \begin{bmatrix} 3C_1+C_2 & C_1+C_2 & & & 0 \\ C_1+C_2 & C_1+6C_2+C_3 & C_2+C_3 & & \\ & \ddots & \ddots & \ddots & \\ & C_{n-2}+C_{n-1} & C_{n-2}+6C_{n-1}+C_n & C_{n-1}+C_n & \\ 0 & & C_{n-1}+C_n & C_{n-1}+3C_n & \end{bmatrix} \tag{26b}$$

$$\{F\} = \frac{1}{2} \begin{Bmatrix} -K_1-K_2 \\ K_1-K_3 \\ \vdots \\ K_{n-2}-K_n \\ K_{n-1}+K_n \end{Bmatrix} + \begin{Bmatrix} q_o \\ 0 \\ \vdots \\ 0 \\ -q_\ell \end{Bmatrix} \tag{26c}$$

It should be noted that in the above expansions of the coefficient matrices the nodal distances (Δx) were assumed to be the same for all elements. If Δx varies from element to element, the derivation of these matrices remains essentially the same except that the resulting expressions become much more complicated.

Another possible approach for evaluating the integrals of Eq. (13) would be through the use of a numerical integration method (for example by using Gaussian quadrature). For this purpose the pressure head h is first evaluated at each numerical integration point by using an expansion similar

to Eq. (20). The values of K and C at the integration points follow then immediately from the functional relations K(h) and C(h). When this approach is followed, the integration, obviously, must be carried out during each iteration within each time step.

The first approach was followed in conjunction with linear finite elements, since this approach resulted in a computationally much more efficient scheme, while the accuracy remained approximately the same. Similar expansions using Hermitian basis functions, however, resulted in rather poor results. Each of the following three expansions of the hydraulic conductivity were attempted for the Hermitian finite element scheme (similar expansions were used for C)

Method 1: Complete Hermitian interpolation.

$$\hat{K}(\xi) = K_1 \phi^1_{01}(\xi) + K_2 \phi^1_{02}(\xi) + \frac{dK_1}{dx} \phi^1_{11}(\xi) + \frac{dK_2}{dx} \phi^1_{12}(\xi) \qquad (27)$$

Method 2: Restricted Hermitian interpolation.

$$\hat{K}(\xi) = K_1 \phi^1_{01}(\xi) + K_2 \phi^1_{02}(\xi) \qquad (28)$$

Method 3: Linear interpolation.

$$\hat{K}(\xi) = K_1 \phi^0_1(\xi) + K_2 \phi^0_2(\xi) \qquad (29)$$

Method 1 generated acceptable results only when extremely small values of Δx and Δt were used during the calculations [Note that in (27) $(\frac{dK}{dx})$ must be expanded as $(\frac{dK}{dh})$ $(\frac{dh}{dx})$]. Severe oscillations were generally

present in the vicinity of the moisture front, especially when infiltration in dry soil was simulated. Method 2 generated fairly acceptable results, while the computational speed for execution of several test problems was much faster than for method 1. However, the calculated moisture fronts usually lagged behind the correct front, leading to unacceptable mass balance errors. At the same time the front itself became severely smeared, especially when simulating infiltration in dry soil. Method 3 generated results which were consistently worse than those obtained with method 2 (i.e., a smeared front and large material balance errors). Because of the poor results obtained with each of the three expansions given above, no further attempts were made to find closed-form integrations by means of suitable alternative expansions for K and C over each local element.

Consequently, numerical techniques were used to evaluate the integrals in (13) in the case of Hermitian basis functions. Several numerical integration schemes are available for this purpose, such as Gaussian or Lobatto integration (see Eq. 25.4.29 and 25.4.32 of Abramowitz and Stegun[51], respectively). Table 1 summarizes the different integration schemes studied in this paper. While a Gaussian integration scheme is probably the most accurate one for a given number of integration points, it does not take full advantage of the properties of the Hermitian basis functions. Inspection of these functions (Fig. 1) shows that they become zero at one (ϕ^1_{0j}) or both corner nodes (ϕ^1_{1j}). The computational effort can hence be reduced by locating some of the integration points at these nodes ("Lobatto" integration). The following example demonstrates this. Using a four-point Lobatto integration scheme (k=4 in Table 1), the following expansion for matrix [B] (Eq. 13b) results (as applied to the first element only).

Table 1 . List of numerical integration formula used in this study.

A. *Gaussian integration.*

$$\int_{-1}^{1} f(\xi)\,d\xi = \sum_{i=1}^{k} w_i f(\xi_i) + E$$

k	$\pm\xi_i$	w_i	E
2	0.5773503	1.0000000	$\frac{1}{135}\frac{\partial^4 f}{\partial \xi^4}$
3	0.0000000 0.7745967	0.8888889 0.5555556	$\frac{1}{15750}\frac{\partial^6 f}{\partial \xi^6}$
4	0.3399810 0.8611363	0.6521452 0.3478548	$\frac{1}{3472875}\frac{\partial^8 f}{\partial \xi^8}$

B. *Lobatto integration.*

$$\int_{-1}^{1} f(\xi)\,d\xi = \frac{2}{k(k-1)}\,[f(-1) + f(1)] + \sum_{i=3}^{k} w_i f(\xi_i) + E$$

k	$\pm\xi_i$	w_i	E
3	1.0000000 0.0000000	0.3333333 1.3333333	$\frac{-1}{30}\frac{\partial^4 f}{\partial \xi^4}$
4	1.0000000 0.4472136	0.1666667 0.8333333	$\frac{-2}{23625}\frac{\partial^6 f}{\partial \xi^6}$
5	1.0000000 0.6546537 0.0000000	0.1000000 0.5444444 0.7111111	$\frac{-1}{2778300}\frac{\partial^8 f}{\partial \xi^8}$

$$[B_{ij}] = \int_0^{\Delta x} C\,\phi_j\,\phi_i\,dx$$

$$= \frac{\Delta x}{2} \int_{-1}^{1} C\,\phi_j\,\phi_i\,d\xi$$

$$\simeq \frac{\Delta x}{2} \sum_{k=1}^{4} w_k\,C_k\,\phi_{jk}\,\phi_{ik}$$

$$= \frac{\Delta x}{2} \sum_{k=2}^{3} w_k\,C_k\,\phi_{jk}\,\phi_{ik} + \begin{cases} \frac{\Delta x}{12}\,C_1 & (i = j = 1) \\ \frac{\Delta x}{12}\,C_4 & (i = j = 3) \\ 0 & (\text{all other } i,j) \end{cases} \qquad (30)$$

where the subscript k refers to evaluation at the k-th integration point. Similar expansions can be obtained for the remaining integrals in (13).

An alternative finite element formulation may be developed based on the lumped-mass approach. This approach was first used by Neuman[28] to speed up numerical convergence when simulating infiltration into extremely dry soil. Mass-lumping is achieved by defining the nodal values of the time derivative as weighted averages over the entire flow region, as follows

$$\int_0^{\ell} C\,\frac{\partial h}{\partial t}\,\phi_i\,dx = \frac{\partial H_i}{\partial t} \int_0^{\ell} C\,\phi_i\,dx. \qquad (31)$$

Application of Eq. (31) will lead to a different coefficient matrix for the time derivative (matrix B, Eq. 13b). For example, for linear finite elements one obtains in this way

$$[B] = \frac{\Delta x}{6}\begin{bmatrix} 2C_1+C_2 & & & 0 \\ & C_1+4C_2+C_3 & & \\ & & \ddots & \\ & & C_{n-2}+4C_{n-1}+C_n & \\ 0 & & & C_{n-1}+2C_n \end{bmatrix} \tag{32}$$

When comparing Eq. (32) with (26b) it is evident that the diagonal entries of (32) are identical to the row sums of the entries in (26b). This lumping together of the row sums has been referred to as the "lumped matrix", or "lumped mass" approximation. Several other techniques for such "lumping" are available, but these are not considered here.

The linear finite element scheme above may be further simplified by redefining the coefficient matrix (32) as

$$[B] = \Delta x \begin{bmatrix} \frac{1}{2}C_1 & & & 0 \\ & C_2 & & \\ & & \ddots & \\ & & C_{n-1} & \\ 0 & & & \frac{1}{2}C_n \end{bmatrix} \tag{33}$$

In this way, a finite difference scheme is obtained. This is easily verified by expanding Eq. (15) for an arbitrary i-th node:

$$a\, h_{i-1}^{t+\Delta t} + b\, h_{i}^{t+\Delta t} + c\, h_{i+1}^{t+\Delta t} = f \tag{34}$$

with

$$a = \frac{-\omega}{2\Delta x}\,(K_{i-1} - K_i) \tag{35a}$$

$$b = \frac{\Delta x}{\Delta t}\,C_i + \frac{\omega}{2\Delta x}\,(K_{i-1}+2K_i+K_{i+1}) \tag{35b}$$

$$c = \frac{-\omega}{2\Delta x}\,(K_i + K_{i+1}) \tag{35c}$$

$$f = -h_{i-1}^{t}\left[\frac{(\omega-1)}{2\Delta x}\,(K_{i-1}+K_i)\right] - h_{i+1}^{t}\left[\frac{(\omega-1)}{2\Delta x}\,(K_i+K_{i+1})\right]$$

$$+h_i^{t}\left[\frac{\Delta x}{\Delta t}\,C_i + \frac{(\omega-1)}{2\Delta x}\,(K_{i-1}+2K_i+K_{i+1})\right] + \frac{1}{2}\,(K_{i-1}-K_{i+1}). \tag{35d}$$

3. *RESULTS*

Two example problems will be presented in this section. The first one concerns the often quoted field infiltration experiment by Warrick *et al.*[52] (see also Segol[46], Bresler[53], Ungs *et al.*[54], Gureghian *et al.*[55]). The experiment is simulated using each of the four numerical schemes discussed in the previous section, i.e., finite differences, linear finite elements, mass-lumped linear finite elements, and Hermitian finite elements. The second example describes the infiltration and redistribution of water in a non-homogeneous (and layered) soil profile. Results for this example were obtained with the Hermitian finite element code (UNSAT1), listed in the appendix.

3.1. *Example 1: The infiltration experiment of Warrick et al.*

In this example (Warrick *et al.*[52]) water is allowed to infiltrate into a 125 cm deep, homogeneous soil profile having the following soil-hydraulic properties:

$$\theta(h) = \begin{cases} 0.6829 - 0.09524 \ln(|h|) & h \leq -29.484 \\ 0.4531 - 0.02732 \ln(|h|) & -29.484 < h \leq -14.495 \end{cases} \tag{36a}$$

$$K(h) = \begin{cases} 19.34\ 10^{4}\ |h|^{-3.4095} & h \leq -29.484 \\ 516.8\ |h|^{-0.97814} & -29.484 < h \leq -14.495 \end{cases} \tag{36b}$$

where the hydraulic conductivity is given in cm/day and h in cm. The

following initial and boundary conditions are adopted

$$\theta(x,0) = \begin{cases} 0.1500 + 0.0008333\ x & 0 < x < 60 \\ 0.2000 & 60 < x \leq 125 \end{cases} \qquad (37a)$$

$$h(0,t) = -14.495 \qquad (\theta_o = 0.38) \qquad (37b)$$

$$h(125,t) = -159.19 \qquad (\theta_\ell = 0.20) \qquad (37c)$$

The initial condition (37a) shows that the moisture content increases linearly between x=0 and x=60 cm. The equivalent pressure distribution at t=0 follows immediately from (37a) by making use of the soil moisture retention curve (Eq. 36a).

The present example was used to evaluate the accuracy and efficiency of the four numerical techniques discussed above, i.e., finite differences (FD), linear finite elements (LFE), mass-lumped (linear) finite elements (MFE) and Hermitian finite elements (HFE). Different numerical integration methods were, furthermore, used to evaluate the integrals in the final matrix equation (Eq. 13) in the case of Hermitian finite elements. Table 2 gives a summary of the various computer runs, including a comparison of the execution (C.P.U.) times needed to complete the simulation on an IBM 360/91 computer (execution was terminated after 0.4 days of infiltration). Computed moisture distributions versus depth are presented in Fig. 2 - 6. The solid line in each case represents the assumed "correct" solution, and was obtained by using increasingly smaller spatial and time increments until all four schemes (FD, LFE, MFE, and HFE) generated essentially the same results.

Table 2. Summary of numerical experiments for example 1 (θ_o=0.38 cm^3/cm^3).

Method *	spatial increment Δx (cm)	number of elements NE -	iteration tolerance TOL (cm)	number of time steps ISTEP -	execution time - (sec)
FD	.50	250	.50	459	41.70
FD	1.00	125	.50	326	15.32
FD	2.50	50	.50	176	3.73
FD	5.00	25	.50	108	1.44
FD	2.50	50	.10	279	6.22
FD	2.50	50	.25	212	4.54
FD	2.50	50	.50	176	3.73
FD	2.50	50	1.00	146	3.27
FD	2.50	50	2.50	116	2.64
FD	2.50	50	.50	176	3.73
LFE	2.50	50	.50	170	3.86
MFE	2.50	50	.50	174	3.82
5LP	5.00	25	.50	156	9.41
2GP	5.00	25	.50	132	6.60
3GP	5.00	25	.50	170	9.91
4GP	5.00	25	.50	149	10.19
4LP	5.00	25	.50	145	7.92
5LP	5.00	25	.50	156	9.41
5LP	5.00	25	.50	156	9.41
5LP	5.00	25	1.00	133	8.52
5LP	5.00	25	2.50	105	6.89
5LP	5.00	25	.50	156	9.41
5LP	7.50	17	.50	118	4.98
5LP	10.00	13	.50	94	3.30

*
FD = Finite Differences
LFE = Linear Finite Elements
MFE = Mass-lumped Linear Finite Elements
2GP = Hermitian Finite Elements (two Gauss points)
3GP = Hermitian Finite Elements (three Gauss points)
4GP = Hermitian Finite Elements (four Gauss points)
4LP = Hermitian Finite Elements (four Lobatto points)
5LP = Hermitian Finite Elements (five Lobatto points)

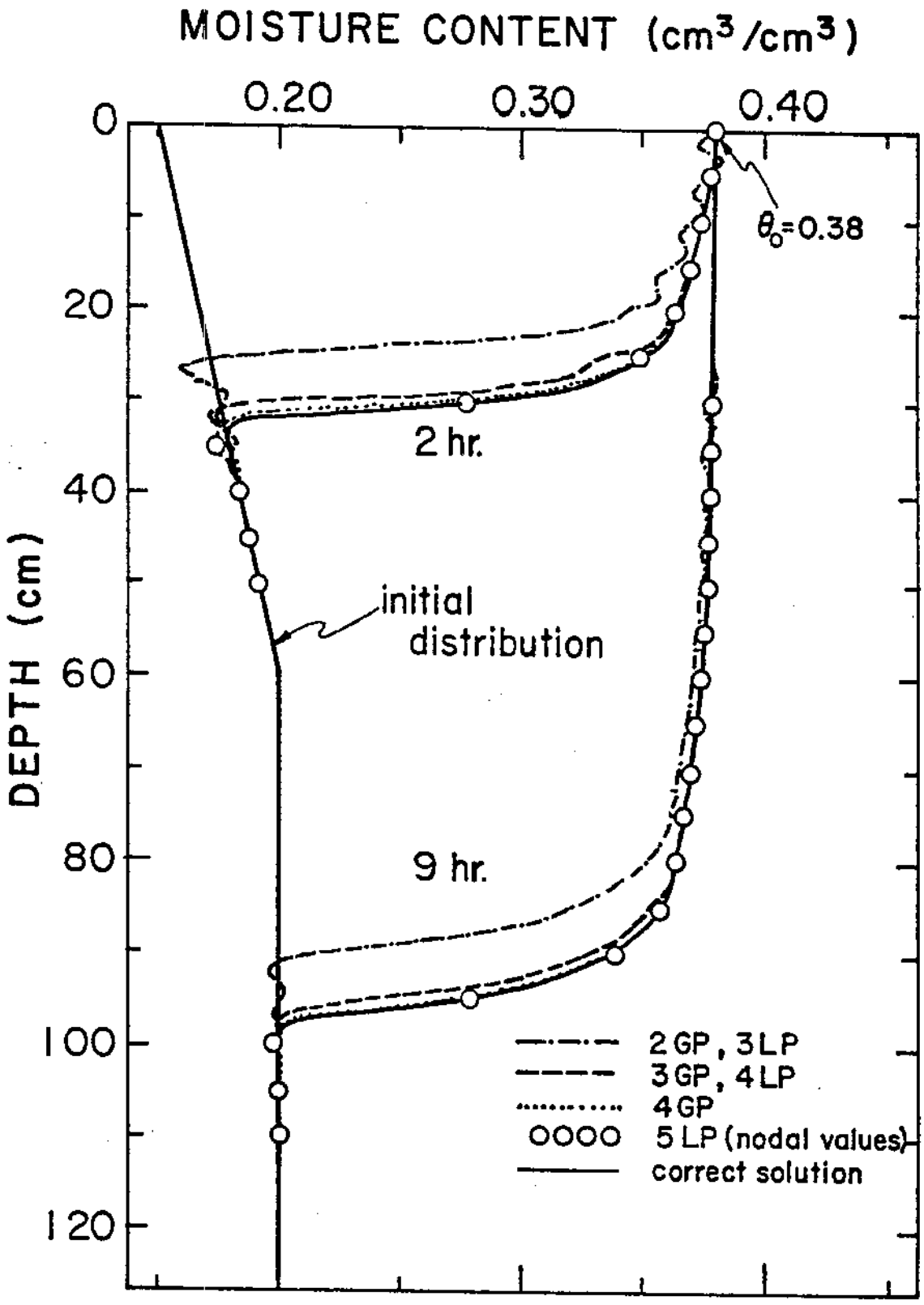

Fig. 2. Effect of different numerical integration schemes on computed moisture profiles, using Hermitian finite elements (example 1).

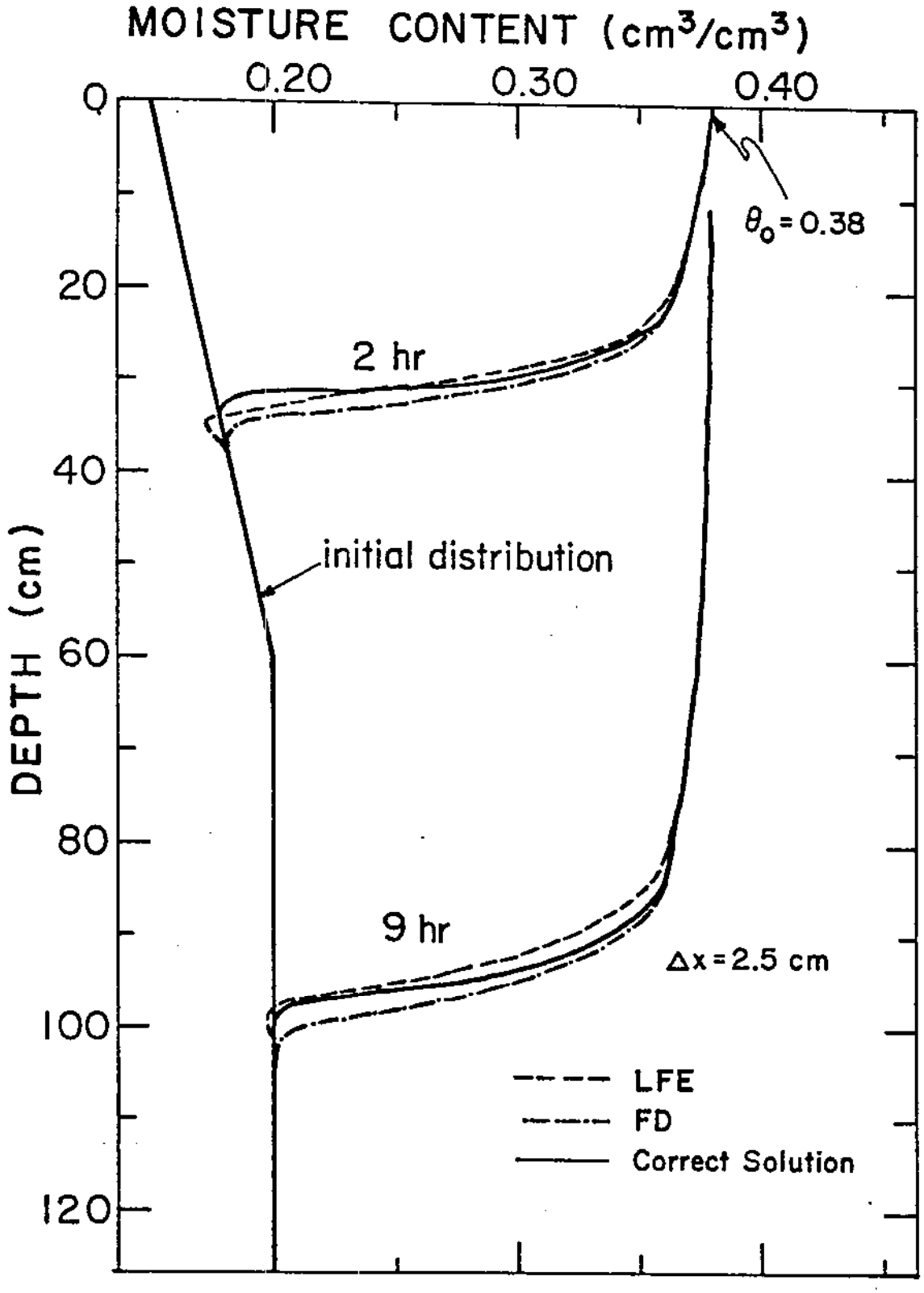

Fig. 3. Moisture content profiles obtained with finite differences (FD) and linear finite elements (LFE) (example 1).

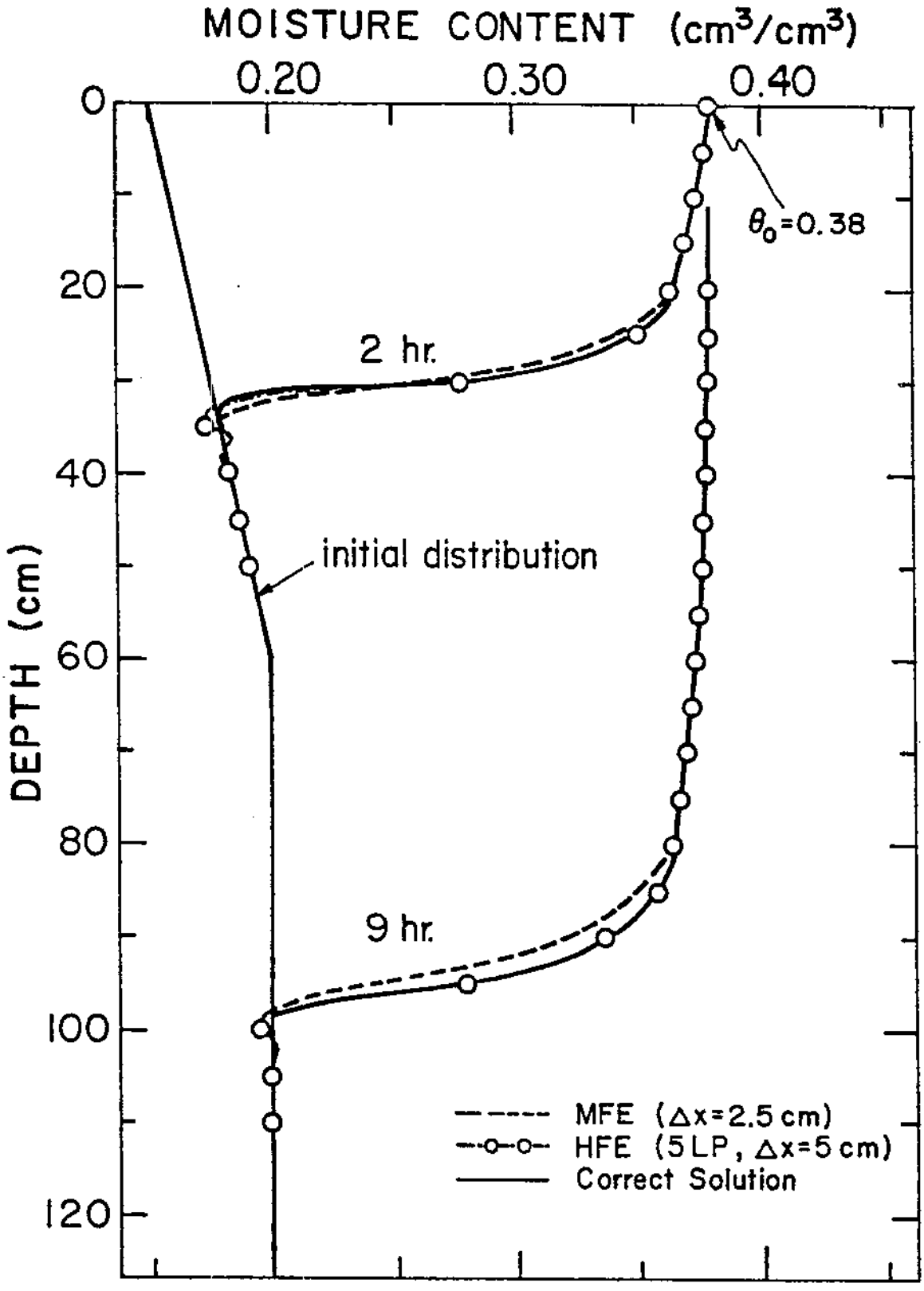

Fig. 4. Moisture content profiles obtained with mass-lumped linear (MFE) and Hermitian finite elements (HFE) (example 1).

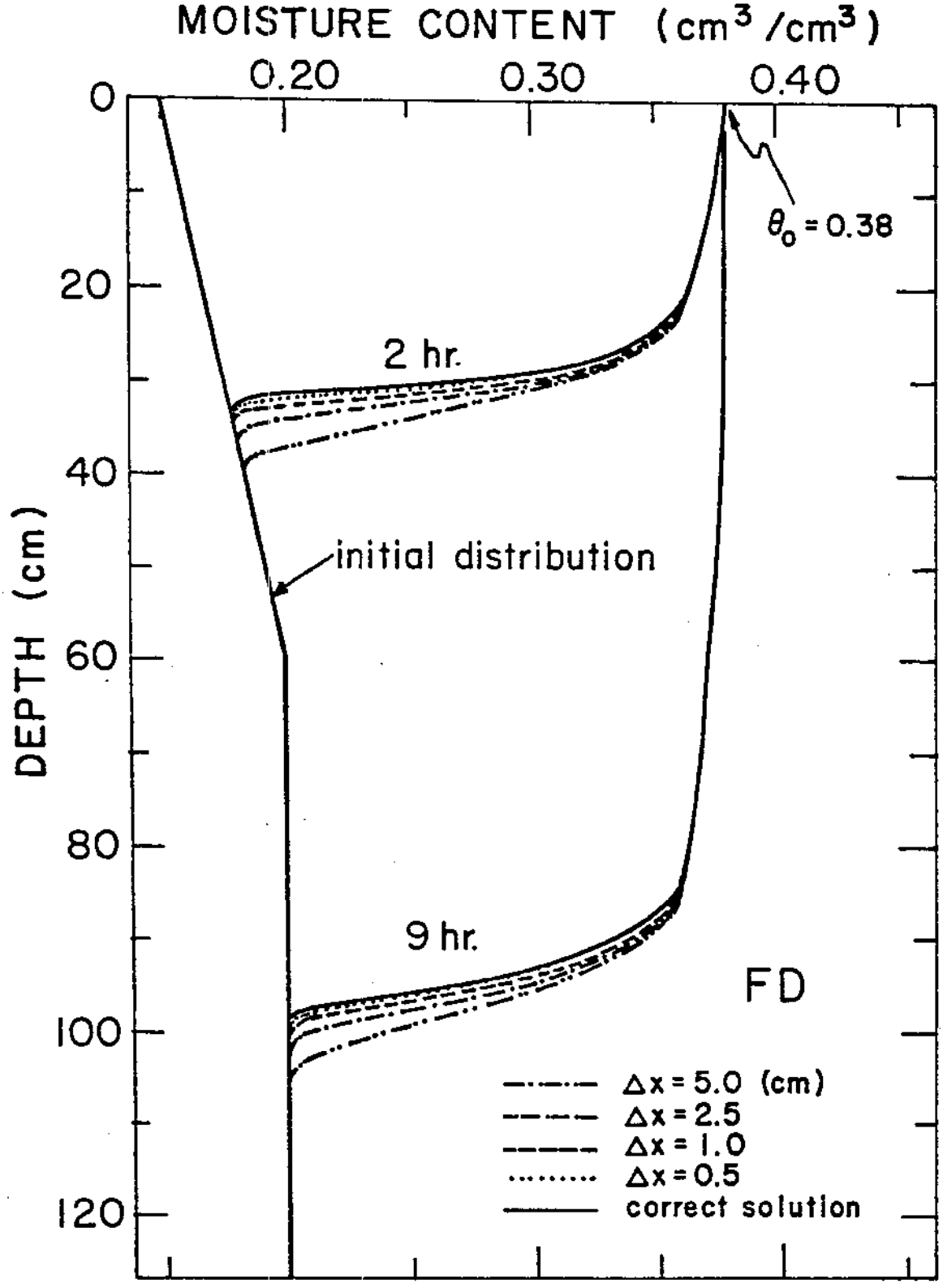

Fig. 5. Effect of nodal spacing on computed moisture profiles using finite differences (example 1).

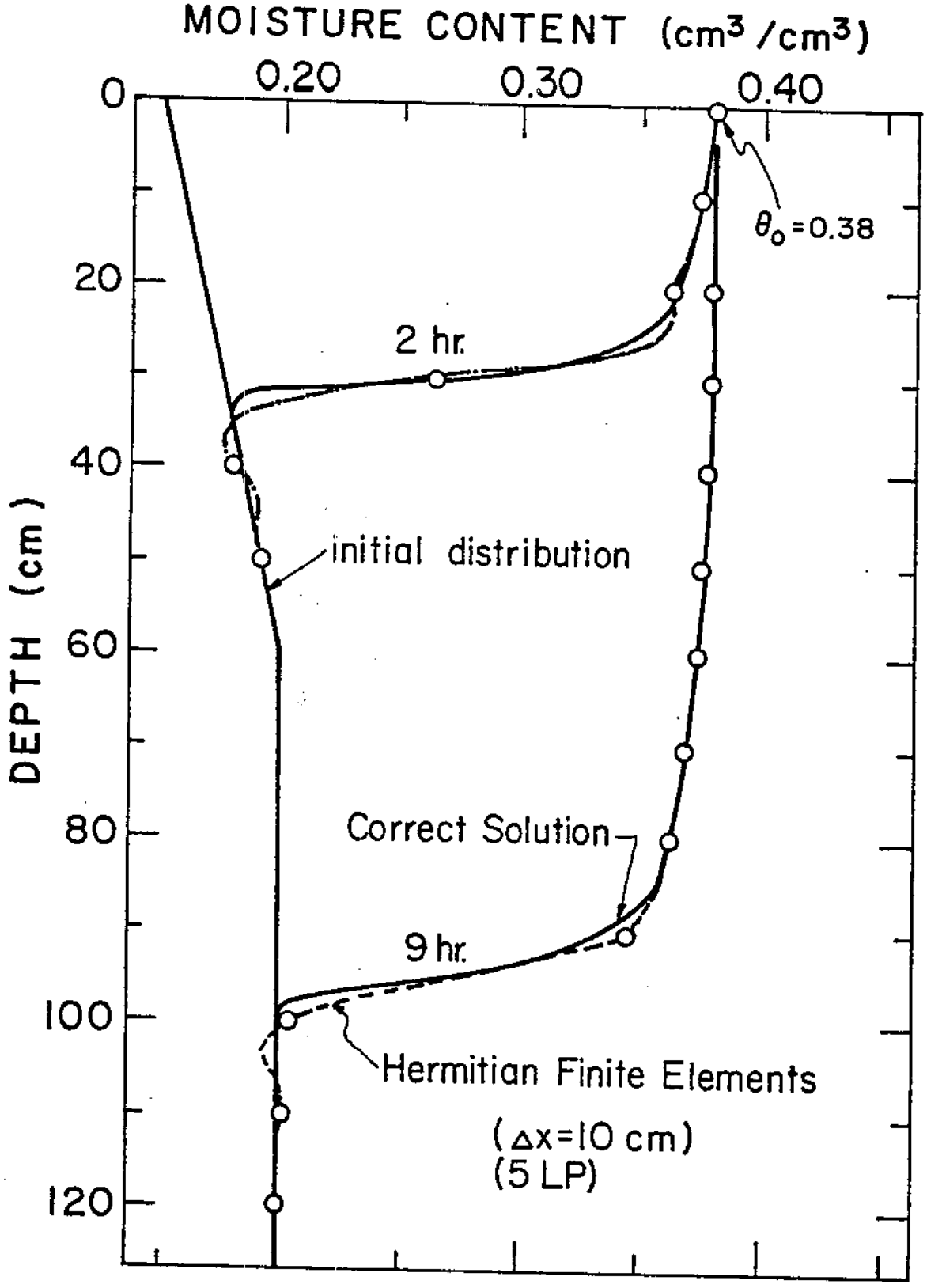

Fig. 6. Comparison of Hermitian finite element solution (Δx=10 cm) with correct solution (example 1).

Results obtained with the various Hermitian finite element schemes are presented in Fig. 2. Each curve was obtained with a different numerical integration scheme. Relatively poor results were generated with the 2-point Gaussian (2GP) and 3-point Lobatto (3LP) integration schemes. The calculated distributions not only lagged considerably behind the correct solution, but also showed some oscillatory behavior near the toe of the moisture fronts, especially during the early stages of infiltration. Much better results were obtained with the 3-point Gaussian (3GP) and 4-point Lobatto (4LP) integration schemes. Also with these schemes, however, the computed distributions lagged somewhat behind the correct solution. The most accurate results were obtained with the 4-point Gaussian (4GP) and 5-point Lobatto (5LP) integration schemes. Actually, the 5LP-scheme generated slightly better results than the 4GP-scheme, even though the execution time for this scheme was less than that for the 3GP-scheme (see Table 2). A nearly exact duplication of the correct solution was obtained with the 5LP-scheme, except near the toe of the moisture front. The small oscillations present here are characteristic for those cases where sharp moisture (and pressure) fronts are simulated. It appears that, at least from a practical point of view, these oscillations are of minor importance, especially if one is aware of the numerical reasons of their presence. Figure 2, furthermore, shows that these oscillations are only significant during the initial stages of infiltration, and that they become smaller in amplitude when the simulation progresses in time.

Results obtained with finite differences (FD) and linear finite elements (LFE) are presented in Fig. 3, while Fig. 4 shows results obtained with mass-lumped linear finite elements (MFE) and Hermitian finite elements

(HFE, 5LP). A constant spatial increment (Δx) of 2.5 cm was used for the three zero-order continuous schemes (FD, LFE, and MFE), while the HFE scheme used a Δx of 5 cm (see also Table 2). Note that the FD- and LFE-schemes generate solutions which deviate slightly from the correct one, and that the computed moisture fronts become somewhat smeared in comparison with the HFE-scheme. Results obtained with the MFE-scheme (Fig. 4) are nearly identical to those obtained with the LFE-scheme (Fig. 5), except near the toe of the computed moisture fronts. No oscillations were observed when mass-lumping was applied to the linear finite element scheme.

While Fig. 3 and 4 demonstrate that the C^1 continuous Hermitian finite element scheme generates the most accurate results, Table 2 also shows that this scheme consumes approximately 2.5 times as much computer time as compared to the various C^0 continuous schemes. The HFE-scheme hence does not immediately present an attractive alternative to the other schemes, unless its relative accuracy does not change dramatically when further increasing the element size. The effects of changing Δx on the computed moisture distributions for FD and HFE are shown in Fig. 5 and 6, respectively. Doubling the spatial increment causes the computed front to move further ahead of the correct solution in the case of FD, while the front itself also becomes more dispersed (smeared). The computer execution time, at the other hand, decreases from 3.7 to 1.5 sec. (Table 2). A doubling of the element size in the HFE-scheme still leads to a fairly accurate description of the moisture front (Fig. 6), although now some more serious oscillations do appear. The computer time in this case is reduced from 9.4 to 3.3 sec.

The values for the execution times given in Table 2 should be viewed

as a first approximation of the efficiency of the different schemes (no claim is made here that each scheme was programmed in the most efficient manner possible). The HFE-scheme uses more computer time than the other schemes for two reasons. First of all, the HFE-scheme generates a matrix equation in which the symmetric coefficient matrices have a full bandwidth of seven (the half-bandwidth is four), while the bandwidth for the three C^0 continuous schemes is only three. Hence, more time is needed for solution of the final matrix equation in the case of Hermitian finite elements. Second, the results given here for HFE were obtained with a simplified version of the program UNSAT1, listed in the appendix. Simplifications were possible by assuming a constant element size and a homogeneous soil profile. The basic setup of the program, however, was kept intact, notably the element by element assembly of the global matrix equation. This method of generating the final matrix equation is rather time consuming and probably not needed when a constant element size is present. Use of the general program UNSAT1 resulted in an execution time of 13.7 sec., as compared to 9.4 sec. for the constant element, homogeneous profile version. Hence, the computer time when using the general version does not seem to increase dramatically.

An accurate comparison of the efficiency of the different schemes is also not easy to obtain because of the many parameters affecting the final results. The results given thus far were obtained with a Crank-Nicolson scheme in time (ω=0.5 in Eq. 14 and 16). Execution times were decreased by approximately 30% when an implicit in time (ω=1.0) scheme was used. Computed moisture distributions in that case, however, generally lagged the correct solution, especially for the C^0 continuous schemes. Important reductions in execution time were also possible by increasing the integra-

tion tolerance parameters (μ_1 and μ_2 in 19). In the above example μ_1 and μ_2 were set to 0.5 cm and 0.0, respectively. Approximately the same results were obtained when μ_1 was varied between 0.1 and 2.5 cm, although in some cases (notably for LFE and HFE) a few minor oscillations were observed in the calculated curves when μ_2 equalled 2.5 cm.

All curves thus far were obtained for a first-type, constant pressure boundary condition at the soil surface (Eq. 37b). Several computer runs were also made for the case where a constant flux is given, i.e., for

$$\left(-K \frac{\partial h}{\partial x} + K\right)\Big|_{x=0} = q_o \tag{38}$$

where q_o is the prescribed flux, assumed to be 37.8 cm/day (i.e., equal to the hydraulic conductivity at a moisture content of 0.38 cm^3/cm^3). Results for FD and HFE are presented in Fig. 7 and 8, respectively. The solid line in both figures again represents the assumed "correct" solution, and was obtained by using increasingly smaller element sizes until all four schemes (FD, LFE, MFE, and HFE) converged to the same solution. Note that the FD solution now does not move ahead of the correct solution, but that the computed moisture front still maintains a slightly dispersed shape as compared to the correct front. Nearly identical results were obtained for the other two zero-order continuous schemes (LFE and MFE). The HFE-scheme again duplicated the correct solution accurately, especially when 4 Gauss points (4GP) or 5 Lobatto points (5LP) were used for the numerical integration. Execution times, when using a flux-type boundary condition, were approximately 25% less than when a first-type boundary condition was used (given that all other conditions remained the same; see Table 2).

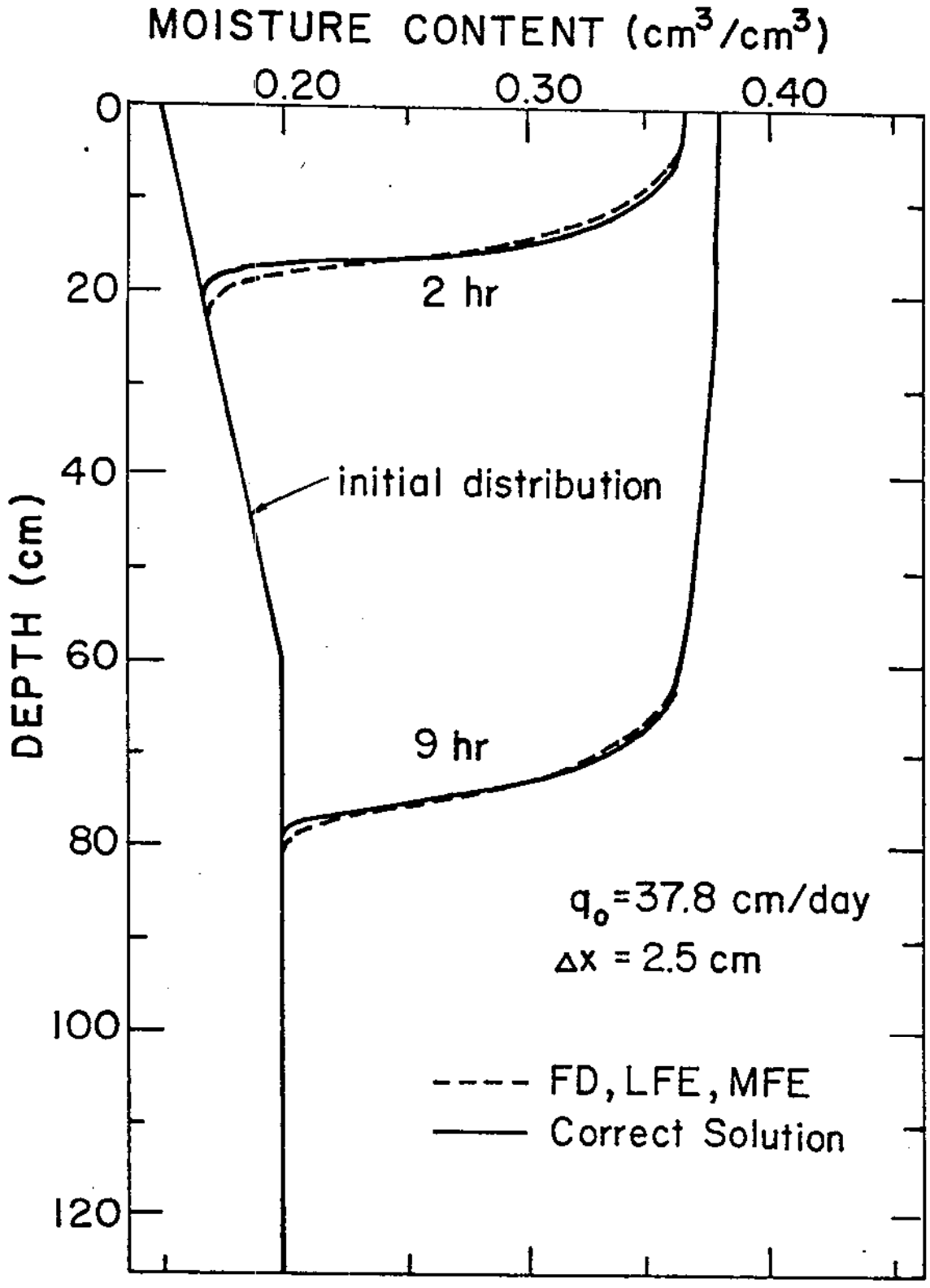

Fig. 7. Comparison of finite differences (FD), linear finite element (LFE) and mass-lumped finite element (MFE) solutions with correct solution (example 1).

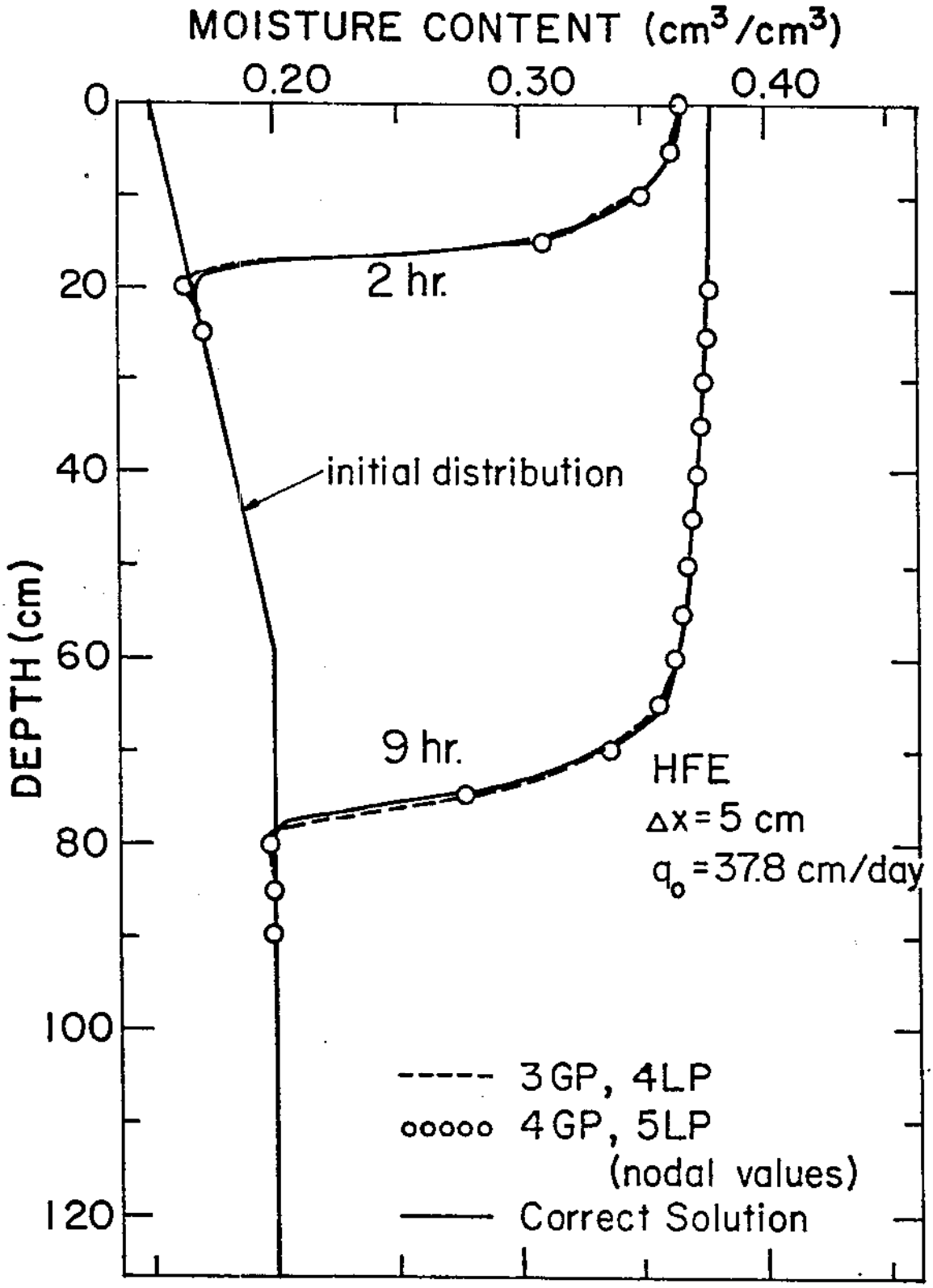

Fig. 8. Comparison of various Hermitian finite element solutions with correct solution (example 1).

From the examples given here and several other numerical experiments it is concluded that the FD- and MFE-schemes will generate the most stable solutions when a steep moisture front is present (e.g., infiltration into a dry, coarse soil). These solutions, however, may diverge somewhat from the correct solutions when the simulation progresses in time, while the calculated moisture front could become more dispersed (smeared out) as compared to the correct front. The HFE-scheme (notably the 5LP-scheme) seems superior in locating the correct spatial location of the moisture front, while the calculated slope of the front is better described than with the various zero-order continuous schemes. However, some oscillations may develop near the toe of the front, especially when relatively large elements are present. If some minor oscillations are allowed, the HFE-scheme appears to become very competitive with the FD- and MFE-schemes. When a flux-type boundary condition can be imposed on the system, much better results are expected for the various C^0-schemes. This suggests that a flux-type boundary condition should be used whenever physically possible.

In many cases, no sharp concentration fronts need to be simulated. In that case the Hermitian finite element scheme becomes very attractive, because much larger elements are allowed in this method. For the more extreme cases, it appears that finite differences and mass-lumped linear finite elements will generate the best results.

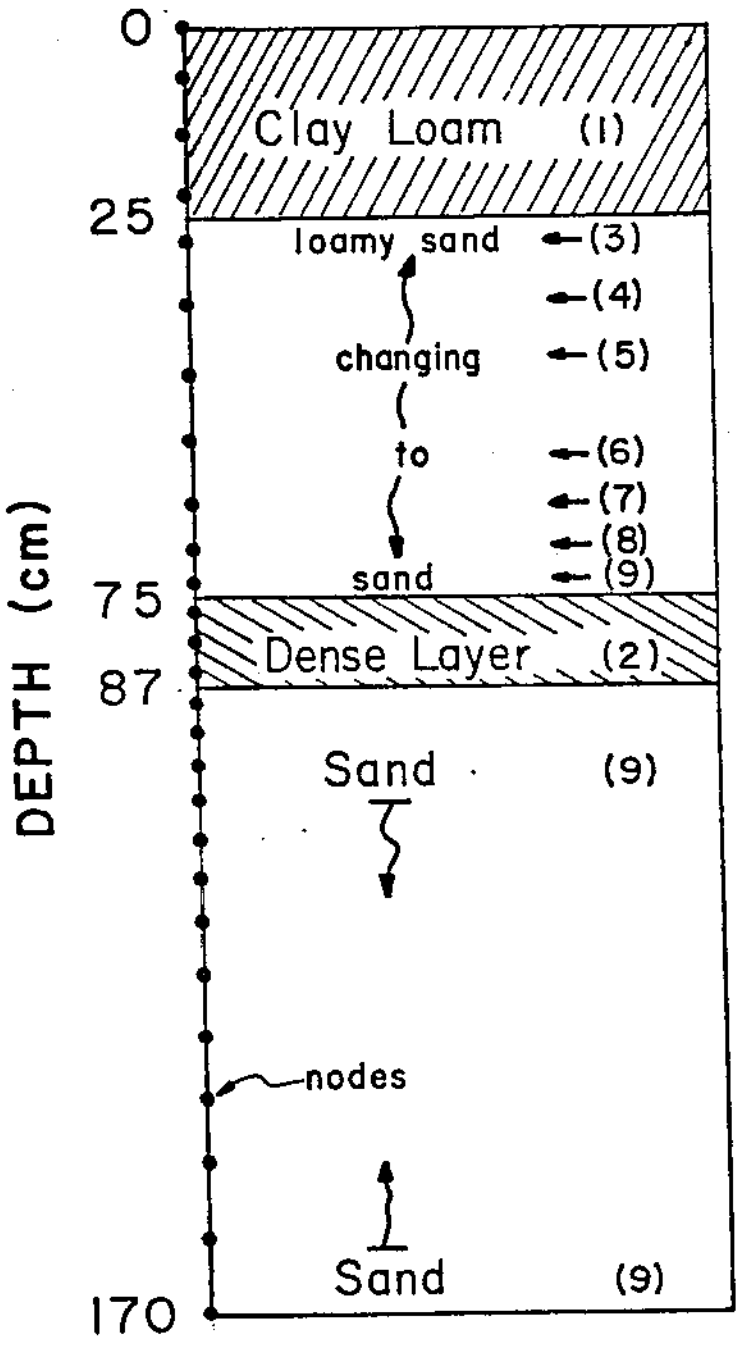

Fig. 9. Schematic cross-section of soil profile used in example 2.

The model for the soil-hydraulic conductivity was obtained by substituting Eq. (39) into the predictive conductivity model of Mualem[57] (Eq. 21 of Mualem). An extensive discussion of Eq. (39) and (40) is given elsewhere[57]. Values of the different parameters appearing in these equations are listed in Table 3 for each soil type used. Figures 10 and 11 present graphical interpretations of some of the resulting curves.

The following initial and boundary conditions are adopted

$$h(x,0) = -350.0 \qquad 0 \leq x \leq 170 \tag{42a}$$

$$\left(-K \frac{\partial h}{\partial x} + K\right)\Big|_{x=0} = \begin{cases} 25.0 & 0 \leq t < 0.50 \\ -0.5 & t \leq 0.50 \end{cases} \tag{42b}$$

$$\frac{\partial h}{\partial x}(170,t) = 0 \qquad t \geq 0. \tag{42c}$$

Before presenting results for this example, it seems necessary to make some observations regarding the non-homogeneous soil properties of the assumed soil profile. Because of the particular properties of the Hermitian finite element scheme, a first-order continuous pressure distribution will be calculated. This makes it necessary that the soil properties change continuously with depth. To clarify this, consider the following example. Suppose the clay loam layer in Fig. 9 would change abruptly into a loamy sand at x=25 cm. Continuity of the soil moisture flux across the interface would then require that

$$q = K_{cl}\left(1 - \frac{\partial h}{\partial x}\right) = K_{ls}\left(1 - \frac{\partial h}{\partial x}\right) \tag{43}$$

Table 3. Constants used to describe the soil-hydraulic properties of the nine soil types of example 2.

Soil No.	θ_r	θ_s	α	n	K_s	S_s
	(cm^3/cm^3)	(cm^3/cm^3)	(cm^{-1})	(-)	(cm/day)	(cm^{-1})
1. (Clay Loam)	.20	.54	.008	1.8	25.	4.10^{-7}
2. (Dense Layer)	.17	.47	.010	2.	75.	5.10^{-8}
3. (Loamy Sand)	.17	.47	.010	2.	75.	1.10^{-7}
4.	.1611	.4611	.01036	2.178	132.8	1.10^{-7}
5.	.15	.45	.0108	2.4	205.	1.10^{-7}
6.	.14	.44	.0112	2.6	270.	1.10^{-7}
7.	.1311	.4311	.01156	2.778	327.8	1.10^{-7}
8.	.1244	.4244	.01182	2.911	371.1	1.10^{-7}
9. (Sand)	.12	.42	.012	3.0	400.	1.10^{-7}

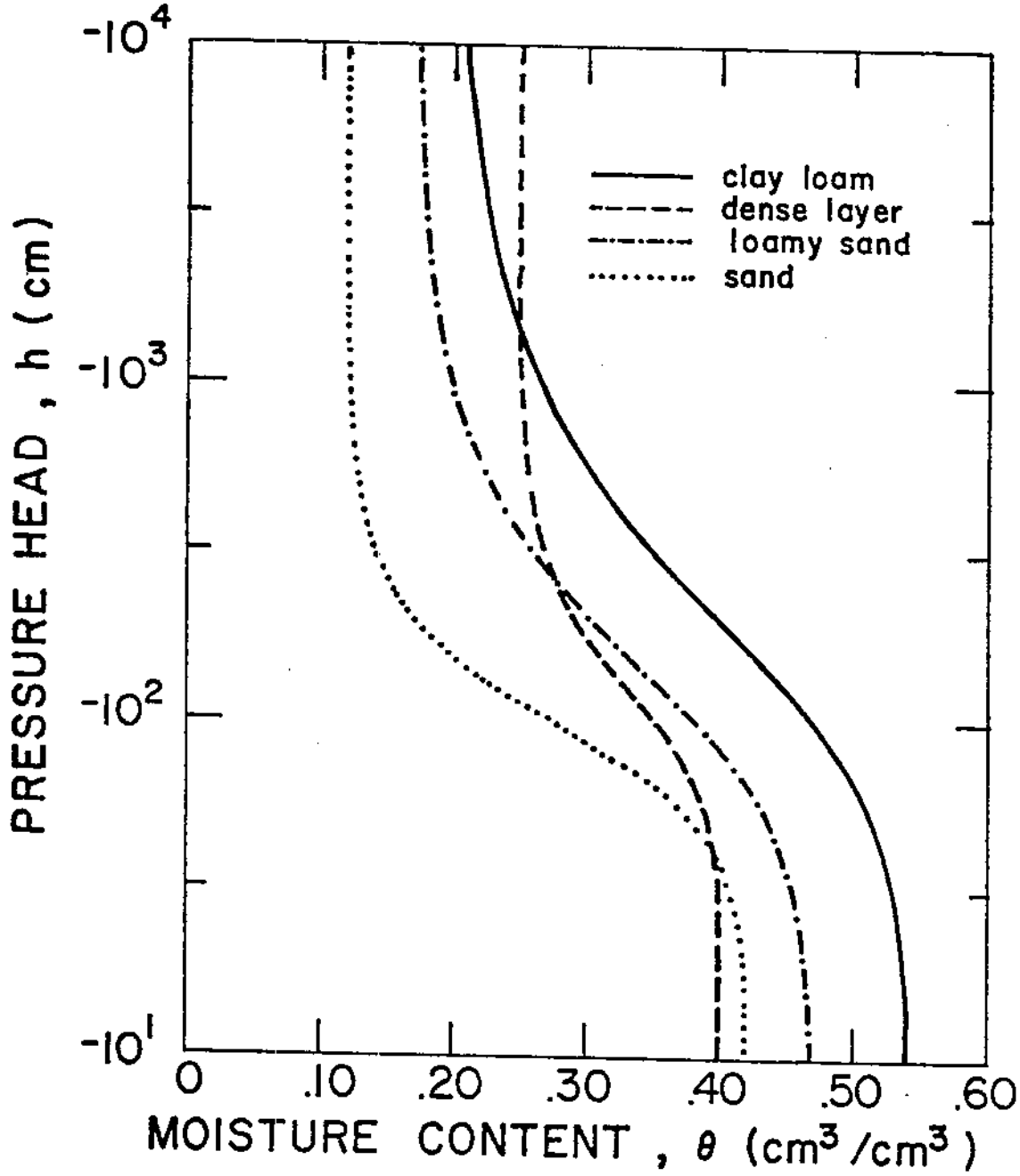

Fig. 10. Soil moisture retention curves of the main soil types used in example 2.

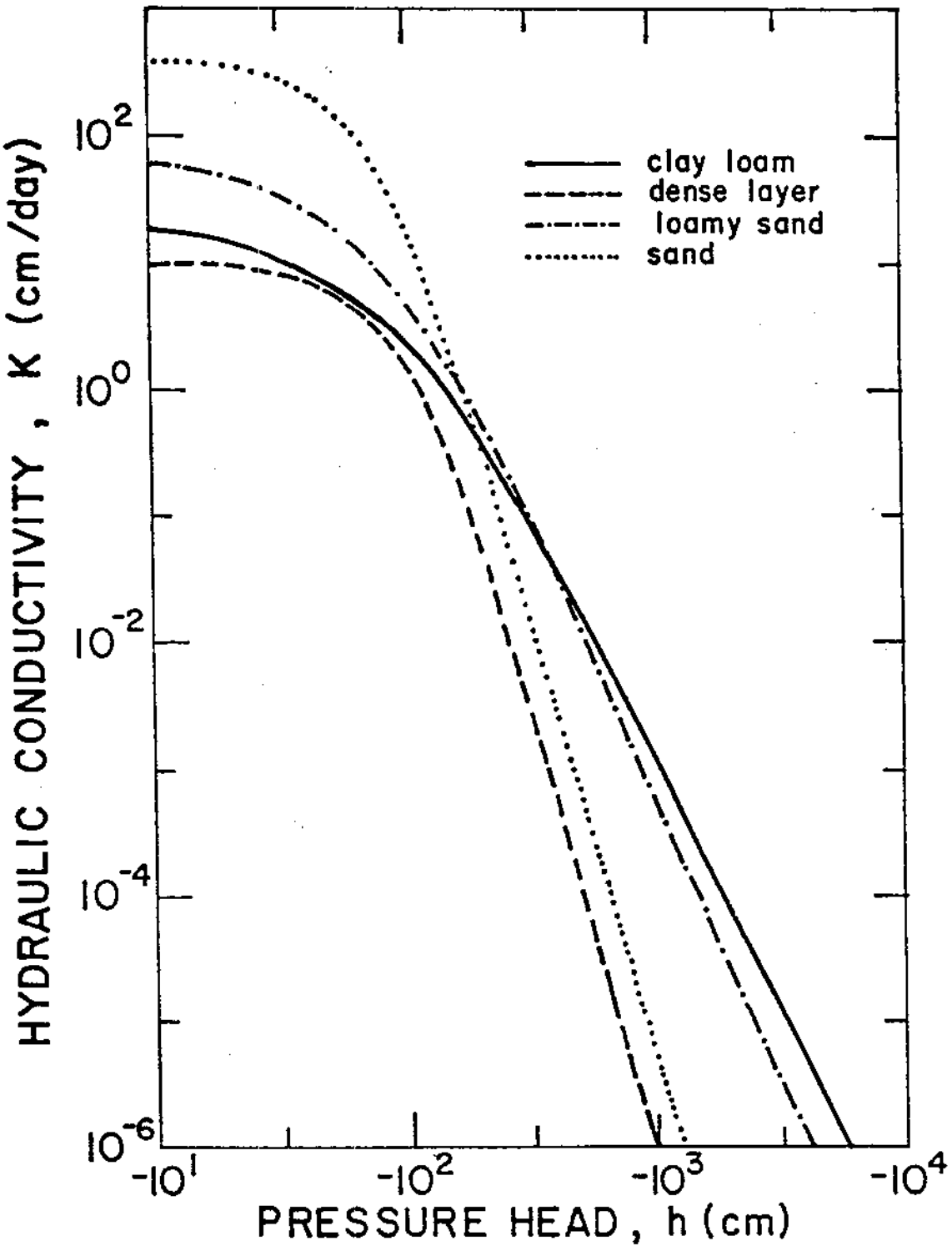

Fig. 11. Predicted hydraulic conductivity curves used in example 2.

where cl and ls indicate evaluation in the clay loam and loamy sand layers, respectively. Because the pressure gradient is continuous across the interface between the two layers, it follows immediately from (43) that also the hydraulic conductivity has to be continuous, i.e., $K_{cl} = K_{ls}$ for all pressure heads. It is clear that this can only be the case if the soil changes in a continuous manner from clay loam to sandy loam. As a result of this the soil moisture content must also change continuously across the boundary between two soil layers.

At least two approaches are possible for modeling the continuous change of one soil material into another. In this study Hermitian basis functions are used to interpolate soil properties between two consecutive nodes when an "abrupt" boundary is present (such as is the case between the clay loam and loamy sand layers at x=25 cm in Fig. 9). Suppose, for example, that the hydraulic conductivity K (or any other soil property) needs to be evaluated between two nodes located at $x=x_1$ and $x=x_2$ (Fig. 12A). Let the conductivity-pressure head curve at x_1 be given by $K_A(h)$, and at x_2 by $K_B(h)$. The pressure head distribution between x_1 and x_2 is given by (see Eq. 23)

$$\hat{h}(x) = \phi_{01}^1(\xi)\ H_1 + \phi_{11}^1(\xi)\ \frac{dH_1}{dx} + \phi_{02}^1(\xi)\ H_2 + \phi_{12}^1(\xi)\ \frac{dH_2}{dx} \qquad (44)$$

where the basis functions $\phi^1(\xi)$ are given by (24), and ξ by (22). The hydraulic conductivity distribution between x_1 and x_2 is now approximated by

$$\hat{K}(x) = \phi_{01}^1(\xi)\ K_A(\hat{h}) + \phi_{02}^1\ K_B(\hat{h}) \qquad (45)$$

Relations similar as (45) for the hydraulic conductivity were also used

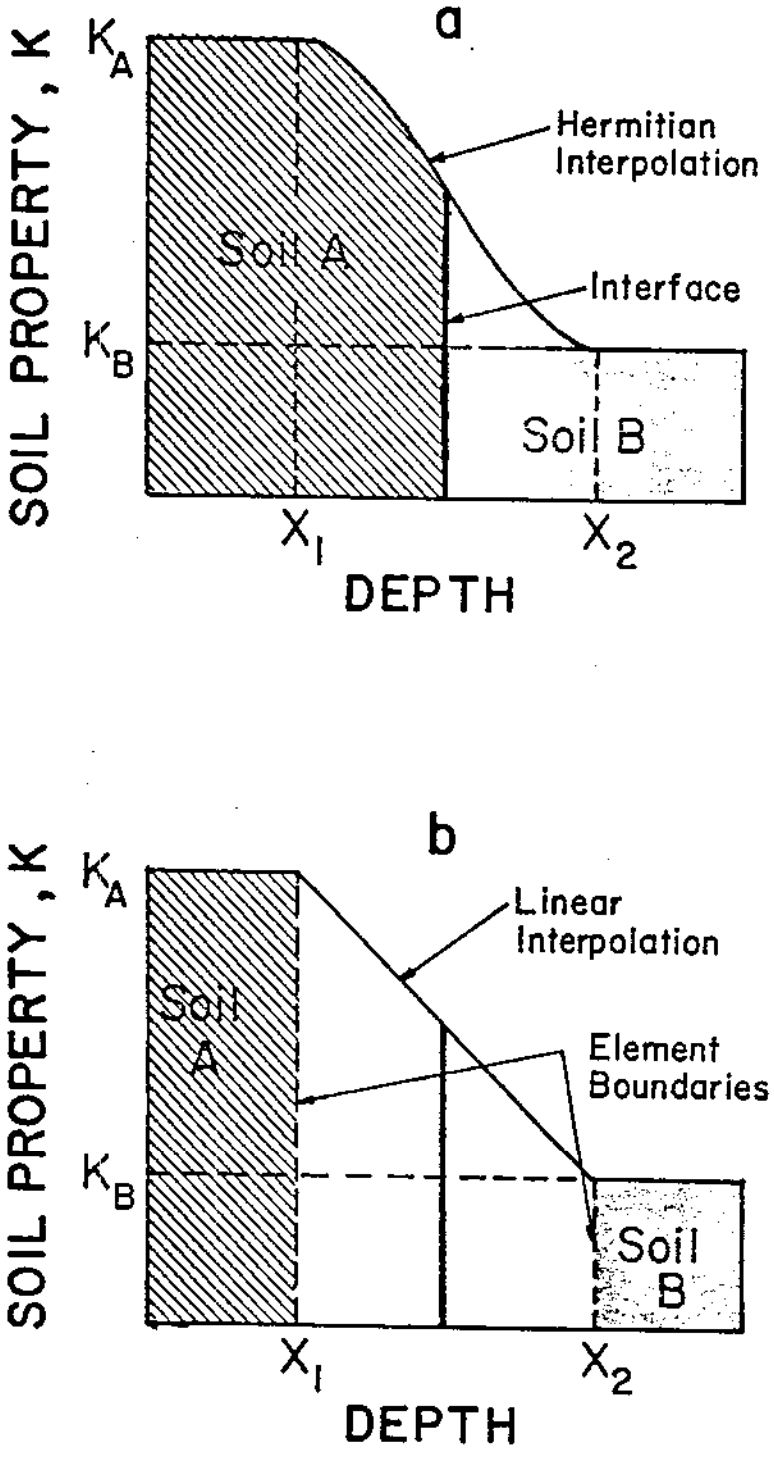

Fig. 12. Schematic representation of the two interpolations used in example 2: a. Restricted Hermitian interpolation for simulation of an "abrupt" boundary; b. Linear interpolation for simulation of smoothly changing soil properties.

for the soil moisture content, $\hat{\theta}(x)$, and the soil moisture capacity, $\hat{C}(x)$.

A slightly different approach is followed when the soil properties change smoothly with depth, such as is the case between x=25 and x=75 cm in Fig. 9. The different parameters (α, n, θ_r, θ_s, and K_s) in Eq. (39) and (40) are assumed to change linearly with depth between x = 28 cm (the first node located in the loamy sand), and x = 73 cm (the node located in the sand). Because of the non-linear properties of (39) and (40), it is not expected that the resulting K(h) and θ(h) curves will also change linearly width depth. In fact, when observed curves are available for any point between 28 and 73 cm, they should be used directly in the calculations. The suggested linear change of the different parameters in (39) and (40) is used here only as a first approximation, and may not be valid in every case. Table 3 lists the resulting parameter values for each node located between the loamy sand and the sand (Soil No. 4 - 8). Each node, hence, has its own characteristic θ(h) and K(h) curve.

The soil-hydraulic properties are also assumed to change linearly *between* two consecutive nodes in the interval between 28 and 73 cm of Fig. 9 (see also Fig. 12B). This linear interpolation is given by

$$\hat{K}(x) = \phi_1^0(\xi)\ K_A(\hat{h}) + \phi_2^0(\xi)\ K_B(\hat{h}) \qquad (46)$$

where the $\phi_j^0(\xi)$ now represent the linear basis functions (Eq. 21).

It should be noted here that the two interpolations given above (Eq. 45 and 46) assume that the soil moisture content and the hydraulic conductivity curves are proportional to the relative amount of each soil material present at any point between two consecutive nodes. This assumption holds also for Eq. (45) since it is assumed there that the soil changes non-

linearly from soil type A to soil type B according to Fig. 12A, i.e., as given directly by the interpolation formula (45). While such a linear relation probably holds for the moisture content, the hydraulic conductivity is not likely to change linearly with the two soil type fractions present. For example, when a mixture is present of 25% clay loam (having a conductivity of K_{cl}) and 75% loamy sand (having a conductivity of K_{ls}), the composite hydraulic conductivity may not necessarily be equal to $0.25\ K_{cl}+0.75\ K_{ls}$. However, because the interpolations are carried out over very short distances (between two consecutive nodes), the resulting errors, if at all present, are likely to be insignificant.

Calculated pressure head distributions versus depth, both for infiltration and redistribution, are presented in Fig. 13 and and 14, while the equivalent moisture distributions are given in Fig. 15 and 16. The calculated pressure distributions remain fairly smooth until the front reaches the dense layer at x=75 cm. The distributions become very steep there, while the pressure gradient immediately above the layer changes its sign from negative to positive. The effect of the dense layer remains clearly visible until the later stages of redistribution (Fig. 14).

As expected, the calculated moisture distributions are much more irregular than the pressure distributions (Fig. 15 and 16). Note that the moisture distributions change very rapidly around x=25 cm (the clay loam-loamy sand boundary) and in the vicinity of the dense layer, but that they remain continuous. The moisture profiles in the interval between 25 and 75 cm become increasingly less steep during infiltration. Figures 15 and 16 also show the distributions of θ_r and θ_s with depth. The calculated moisture distributions always fall between these two curves.

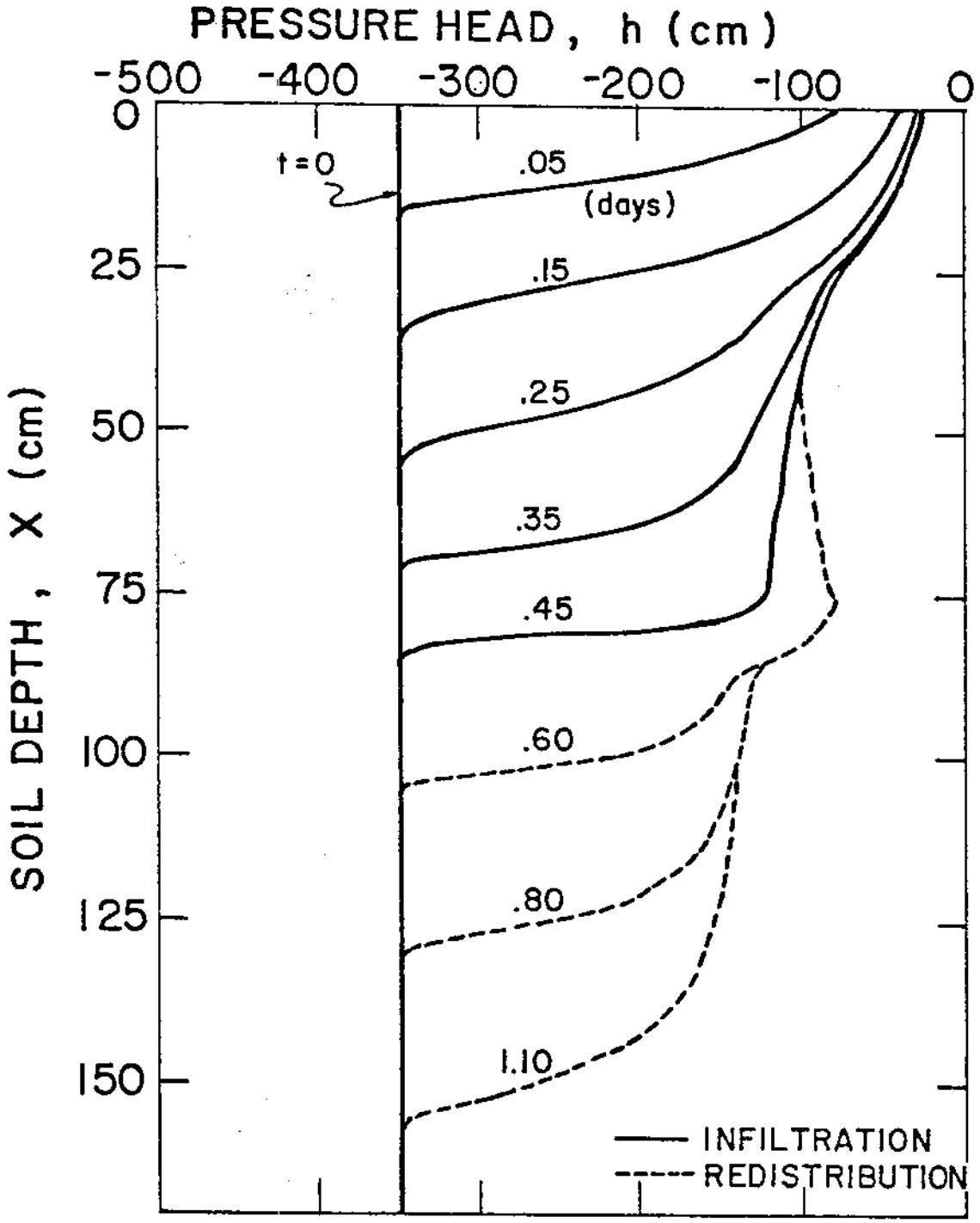

Fig. 13. Calculated pressure distributions during infiltration and the early stage of redistribution (example 2).

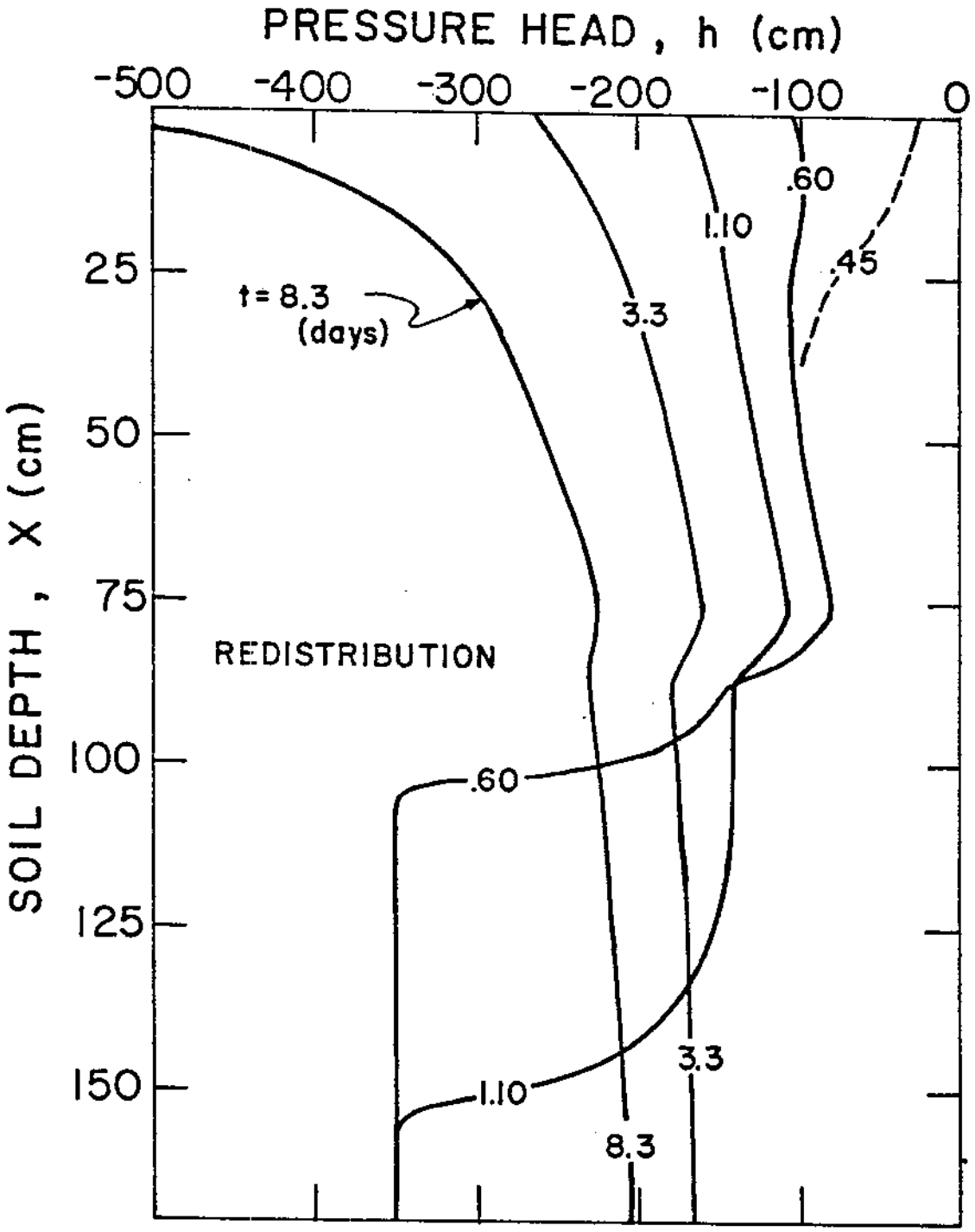

Fig. 14. Calculated pressure distributions during redistribution (example 2).

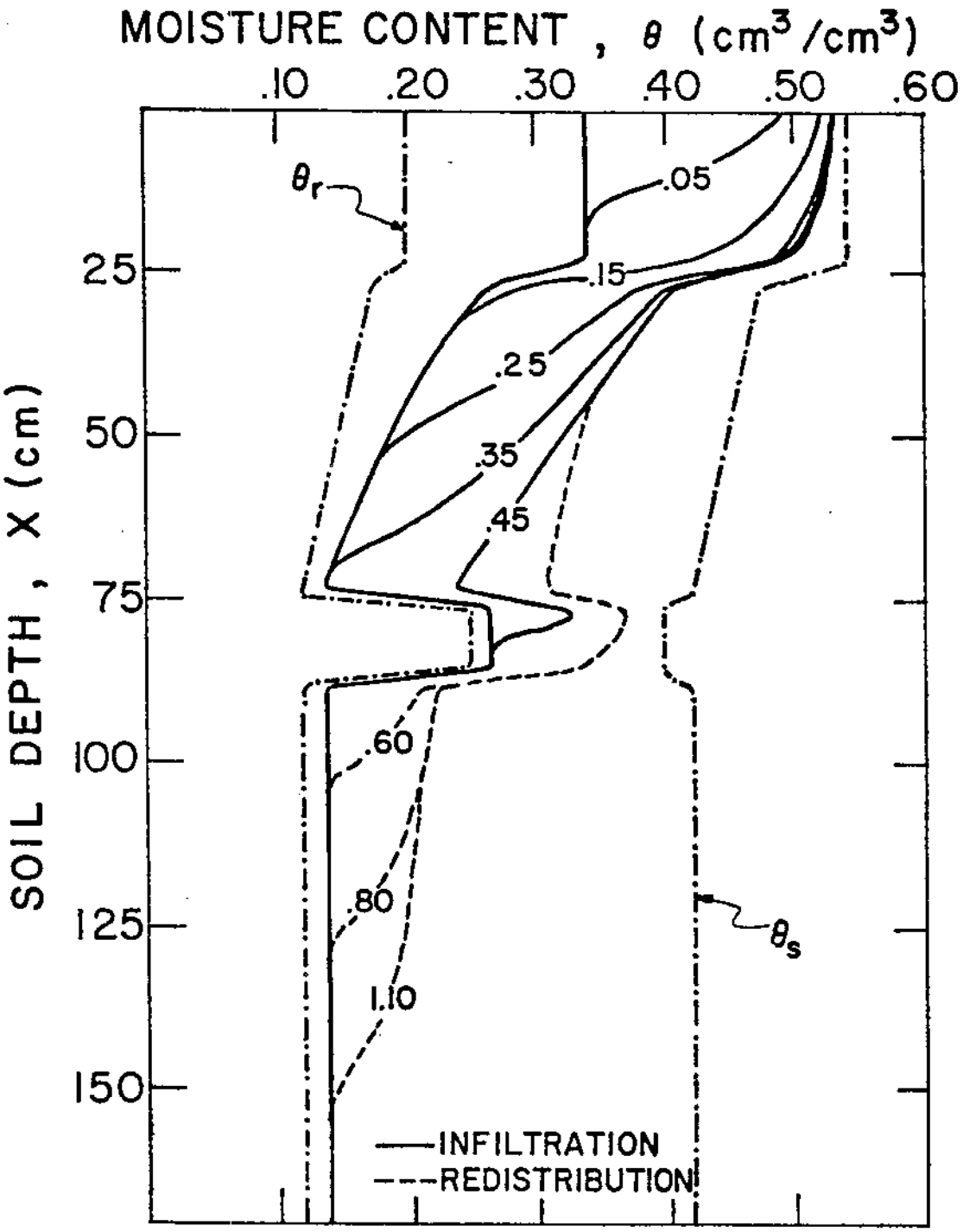

Fig. 15. Calculated moisture content profiles during infiltration and the early stages of redistribution (example 2).

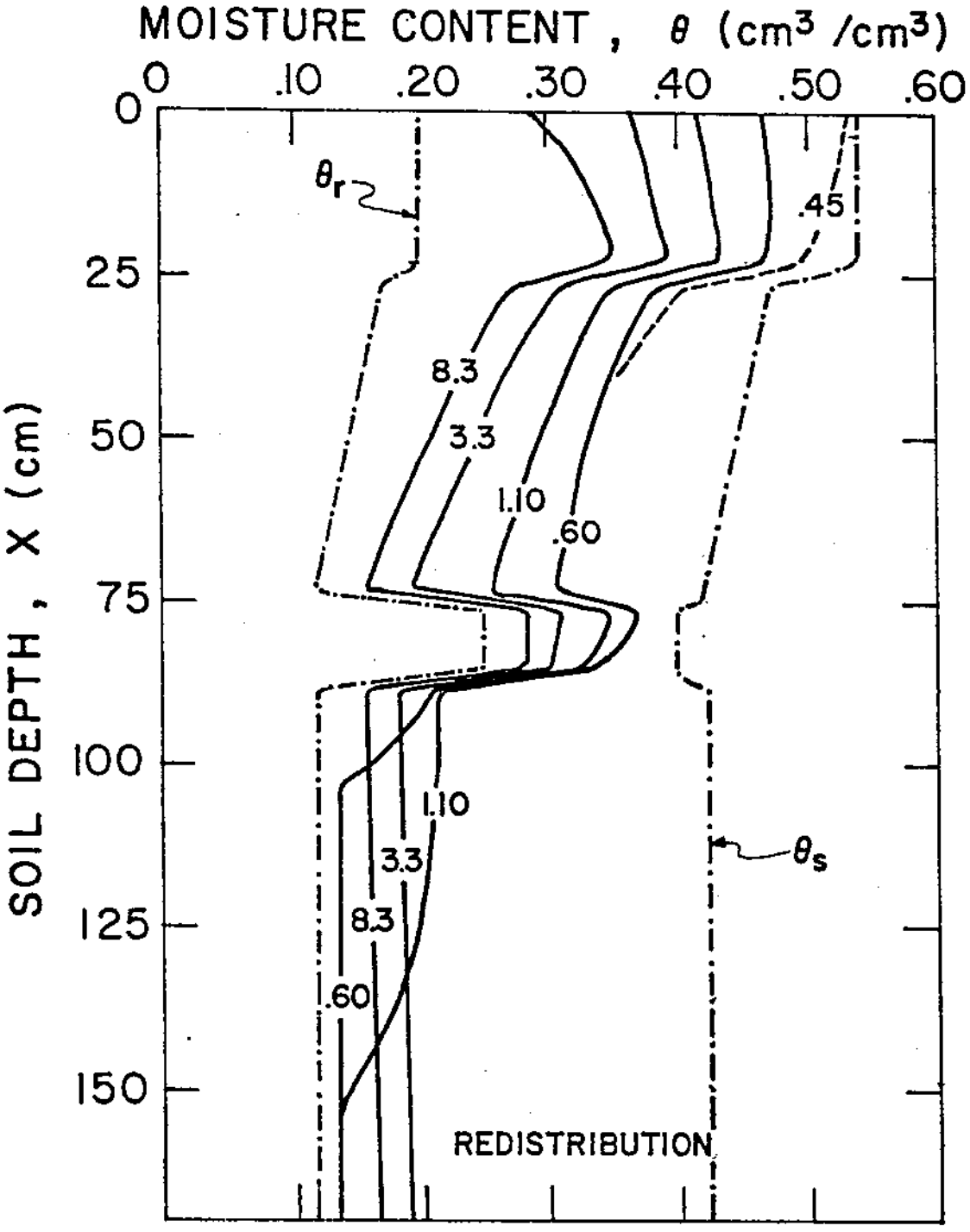

Fig. 16. Calculated moisture content distributions during redistribution (example 2).

REFERENCES

1. Philip, J.R. 1955. Numerical solution of equations of the diffusion type with diffusivity concentration-dependent. I. Trans. Faraday Soc. 51: 885-892.

2. Philip, J.R. 1957. Numerical solution of equations of the diffusion type with diffusivity concentration-dependent. II. Aus. J. Phys. 10: 29-42.

3. Philip, J.R. 1969. Theory of infiltration. Adv. Hydrosci. 5: 215-296. Academic Press, New York.

4. Parlange, J.-Y. 1971a. Theory of water-movement in soils: 1. One-dimensional absorption. Soil Sci. 111(2): 134-137.

5. Parlange, J.-Y. 1971b. Theory of water-movement in soils: 2. One-dimensional infiltration. Soil Sci. 111(3): 170-174.

6. Raats, P.A.C. 1971. Some properties of flows in unsaturated soils with an exponential dependence of the hydraulic conductivity upon the pressure head. J. Hydrol. 14: 129-138.

7. Raats, P.A.C. 1976. Analytical solutions of a simplified flow equation. Trans. ASAE 19(4): 683-689.

8. Warrick, A.W. 1975. Analytical solutions to the one-dimensional linearized flow equation for arbitrary input. Soil Sci. 120(2): 79-84.

9. Warrick, A.W. 1976. Solution for the one-dimensional linear moisture flow equation with implicit water extraction functions. Soil Sci. Soc. Am. J. 40(3): 342-344.

10. Babu, D.K. 1976a. Infiltration analysis and pertubation methods: 2. Horizontal absorption. Water Resour. Res. 12(5): 1013-1018.

11. Babu, D.K. 1976b. Infiltration analysis and pertubation methods: 3. Vertical infiltration. Water Resour. Res. 12(5): 1019-1024.

12. Hanks, R.J., and S.A. Bowers. 1962. Numerical solution of the moisture flow equation for infiltration into layered soils. Soil Sci. Soc. Am. Proc. 26(6): 530-534.

13. Ashcroft, G., D.D. Marsh, D.D. Evans, and L. Boersma. 1962. Numerical method for solving the diffusion equation: I. Horizontal flow in semi-infinite media. Soil Sci. Soc. Am. Proc. 26(6): 522-525.

14. Rubin, J., and R. Steinhardt. 1963. Soil water relations during rain infiltration: I. Theory. Soil Sci. Soc. Am. Proc. 27(3): 246-251.

15. Whisler, F.D., and A. Klute. 1965. The numerical analysis of infiltration, considering hysteresis, into a vertical soil column at equilibrium under gravity. Soil Sci. Soc. Am. Proc. 29(5): 489-494.

16. Klute, A., F.D. Whisler, and E.J. Scott. 1965. Numerical solution of the nonlinear diffusion equation for water flow in a horizontal column of finite length. Soil Sci. Soc. Am. Proc. 29(4): 353-358.

17. Staple, W.J. 1966. Infiltration and redistribution of water in vertical columns of loam soil. Soil Sci. Soc. Am. Proc. 30(5): 553-558.

18. Rubin, J. 1967. Numerical method for analyzing hysteresis-affected, post-infiltration redistribution of soil moisture. Soil Sci. Soc. Am. Proc. 31(1): 13-20.

19. Wang, F.C., and V. Lakshminarayana. 1968. Mathematical simulation of water movement through unsaturated nonhomogeneous soils. Soil Sci. Soc. Am. Proc. 32(3): 329-334.

20. Whisler, F.D., and K.K. Watson. 1969. Analysis of infiltration into draining porous media. J. Irrig. and Drain. Div., ASCE 95(IR4): 481-491.

21. Freeze, R.A. 1969. The mechanism of natural ground-water recharge and discharge. 1. One-dimensional, vertical, unsteady, unsaturated flow above a recharging or discharging ground-water flow system. Water Resour. Res. 5(1): 153-171.

22. Hanks, R.J., A. Klute, and E. Bresler. 1969. A numeric method for estimating infiltration, redistribution, drainage, and evaporation of water from soil. Water Resour. Res. 5(5): 1064-1069.

23. Staple, W.J. 1969. Comparison of computed and measured moisture redistribution following infiltration. Soil Sci. Soc. Am. Proc. 33(6): 840-847.

24. Jeppson, R.W. 1970. Solution to transient vertical moisture movement based upon saturation-capillary pressure data and a modified Burdine theory. Report PRWG-59C-5, Utah Water Res. Lab., Utah State University, Logan, Utah.

25. Green, D.W., H. Dabiri, and C.F. Weinaug. 1970. Numerical modeling of unsaturated groundwater flow and comparison of the model to a field experiment. Water Resour. Res. 6(3): 862-874.

26. Hornberger, G.M., and I. Remson. 1970. A moving boundary model of a one-dimensional saturated-unsaturated, transient porous flow system. Water Resour. Res. 6(3): 898-905.

27. Bhuiyan, S.I., D.A. Hiler, C.H.M. van Bavel, and A.R. Aston. 1971. Dynamic simulation of vertical infiltration into unsaturated soils. Water Resour. Res. 7(6): 1597-1606.

28. Neuman, S.P. 1972. Finite element computer programs for flow in saturated-unsaturated porous media. Second Annual Report, No. A10-SWC-77, Hydraul. Eng. Lab., Technion, Haifa, Israel.

29. van Keulen, H., and G.E.M. van Beek. 1971. Water movement in layered

soils. A simulation model. Neth. J. Agric. Sci. 19: 138-153.

30. Reichardt, K., D.R. Nielsen, and J.W. Biggar. 1972. Horizontal infiltration into layered soils. Soil Sci. Soc. Am. Proc. 36(6): 858-863.

31. Giesel, W., M. Renger, and O. Strebel. 1972. Numerical treatment of the unsaturated flow equation: comparison of experimental and computed results. Water Resour. Res. 9(1): 174-177.

32. Bruch, J.C. Jr., and G. Zyvoloski. 1973. Solution of equation for vertical unsaturated flow of soil water. Soil Sci. 116(6): 417-422.

33. Ahuja, L.R. 1973. A numerical and similarity analysis of infiltration into crusted soils. Water Resour. Res. 9(4): 987-994.

34. Nimah, M.N., and R.J. Hanks. 1973. Model for estimating soil water, plant, and atmospheric interrelations: I. Description and sensitivity. Soil Sci. Soc. Am. Proc. 37(4): 522-527.

35. Debouche, Ch., S. Gaspar, and L. Sine. 1974. Diffusivitè de l'eau dans un milieu non satuře ńeteroǧene. J. Hydrol. 22: 35-51. 1974.

36. van der Ploeg, R.R. 1974. Simulation of moisture transfer in soils: one-dimensional infiltration. Soil Sci. 118(6): 349-357.

37. Bruch, J.C. Jr. 1975. Finite element solutions for unsteady and unsaturated flow in porous media. Techn. Compl. Rep., Contribution No. 151, Calif. Water Resour. Center, Univ. of California, Davis.

38. Hillel, D.I., C.H.M. van Bavel, and H. Talpaz. 1975. Dynamic simulation of water storage in fallow soil as affected by mulch of hydrophobic aggregates. Soil Sci. Soc. Am. Proc. 39(5): 826-833.

39. Dane, J.H., and P.J. Wierenga. 1975. Effect of hysteresis on the prediction of infiltration, redistribution, and drainage of water in a layered soil. J. Hydrol. 25: 229-242.

40. Narasimhan, T.N. 1975. A unified numerical model for saturated-unsaturated groundwater flow. Ph.D. Thesis, Univ. of California, Berkeley, Calif.

41. Finlayson, B.A. 1977. Water movement in desiccated soils. In Finite Elements in Water Resources, W.G. Gray *et al.* (eds.), Pentech Press, London, pp. 3.91-3.106.

42. Haverkamp, R., M. Vauclin, J. Touma, P.J. Wierenga, and G. Vachaud, 1977. A comparison of numerical simulation models for one-dimensional infiltration. Soil Sci. Soc. Am. J. 41(2): 285-294.

43. Hayhoe, H.N. 1978. Study of the relative efficiency of finite difference and Galerkin techniques for modeling soil-water transfer. Water Resour. Res. 14(1): 97-102.

44. Brebbia, C.A., and J.J. Connor. 1974. Fundamentals of Finite Element Techniques for Structural Engineers. Butterworths, London.

45. Pinder, G.F., and W.G. Gray. 1977. Finite Element Simulation in Surface and Subsurface hydrology. Academic Press, New York.

46. Segol, G. 1977. A three-dimensional Galerkin-finite element model for the analysis of contaminant transport in saturated-unsaturated porous media. In Finite Elements in Water Resources, W.G. Gray *et al.* (eds.), Pentech Press, London, pp. 2.123-2.144.

47. Frind, E.O., R.W. Gilham, and J.F. Pickens. 1977. Application of unsaturated flow properties in the design of geologic environments for radioactive waste storage facilities. In Finite Elements in Water Resources. W.G. Gray *et al.* (eds.), Pentech Press, London, pp. 3.133-3.163.

48. Ergatoudis, I., B.M. Irons, and O.C. Zienkiewicz. 1968. Curved isoparametric, 'quadrilateral' elements for finite element analysis. Int. J. Solids Struct., 4: 31-42.

49. Oden, J.T. 1972. Finite Elements of Nonlinear Continua. McGraw-Hill, New York.

50. Zienkiewicz, O.C. 1971. The Finite Element Method in Engineering Science. McGraw-Hill, New York.

51. Abramowitz, M., and I.A. Stegun. 1970. Handbook of Mathematical Functions. Dover Publ., New York.

52. Warrick, A.W., J.W. Biggar, and D.R. Nielsen. 1971. Simultaneous solute and water transfer for an unsaturated soil. Water Resour. Res. 7(5): 1216-1225.

53. Bresler, E. 1973. Simultaneous transport of solutes and water under transient unsaturated flow conditions. Water Resour. Res. 9(4): 975-986.

54. Ungs, M., R.W. Cleary, L. Boersma, and S. Yingjajaval. 1976. The quantitative description of transfer of water and chemicals through soils. In Land as a Waste Management Alternative, R.C. Loehr (ed.), Ann Arbor Sci., Ann Arbor, Michigan, pp. 109-137.

55. Gureghian, A.B., R.W. Cleary, and D.S. Ward. 1977. One-dimensional modeling of unsaturated pollutant transport. Final Report 208 Project, Nassau-Suffolk County Regional Planning Board, Hauppauge, New York.

56. van Genuchten, M.Th. 1978. Calculating the unsaturated hydraulic conductivity with a new, closed-form analytical model. Research Report 78-WR-08, Water Resources Program, Department of Civil Engineering, Princeton University, Princeton, New Jersey.

57. Mualem, Y. 1976. A new model for predicting the hydraulic conductivity of unsaturated porous media. Water Resour. Res. 12(3): 513-522.

APPENDIX

UNSAT1:

A COMPUTER PROGRAM FOR CALCULATING

ONE-DIMENSIONAL SATURATED-UNSATURATED

MOISTURE MOVEMENT IN SOILS.

This appendix gives a brief description and listing of UNSAT1, a computer model for simulating moisture movement in a one-dimensional, saturated-unsaturated and non-homogeneous soil profile. The program consists of a main program (MAIN), four subroutines (DATAIN, MATEQ, BANSOL, and PRINT), and two functions (BC and SPR). The main program controls the sequence of calculations in the model, as schematically shown by the flow chart in Fig. A1. The subroutine DATAIN is first used to read the input data and to define the geometry and initial conditions of the system. In addition, DATAIN may be used to obtain a listing of the different soil-hydraulic properties (controlled by the output code KOD3). The subroutine MATEQ provides the necessary calculations for assembly of the global matrix equation, while the subroutine BANSOL solves this equation for the updated values of the pressure head and its gradient (PE).

A check on the iterative process is subsequently performed in MAIN. If convergence is not met, the iterative process either continues (if NIT<NITMAX), restarts with a smaller DELT (if NIT=NITMAX), or stops altogether (if DELT<DELMIN). If convergence is met, on the other hand, the simulation proceeds in time until either the maximum simulation time is reached (SUMT>TMAX), or a given number of time steps is executed (ISTEP=NSTEPS). Possible output is provided by the subroutine PRINT. This subroutine also computes a cumulative mass balance of the soil profile.

The functions BC and SPR are problem-dependent. BC supplies the transient data for the boundary condition at the soil surface (either a first-type or flux-type boundary condition is given). These data are given in table form. The function SPR, furthermore, generates the different soil-hydraulic functions [$\theta(h)$, $K(h)$, $C(h)$, and $h(\theta)$]. In the

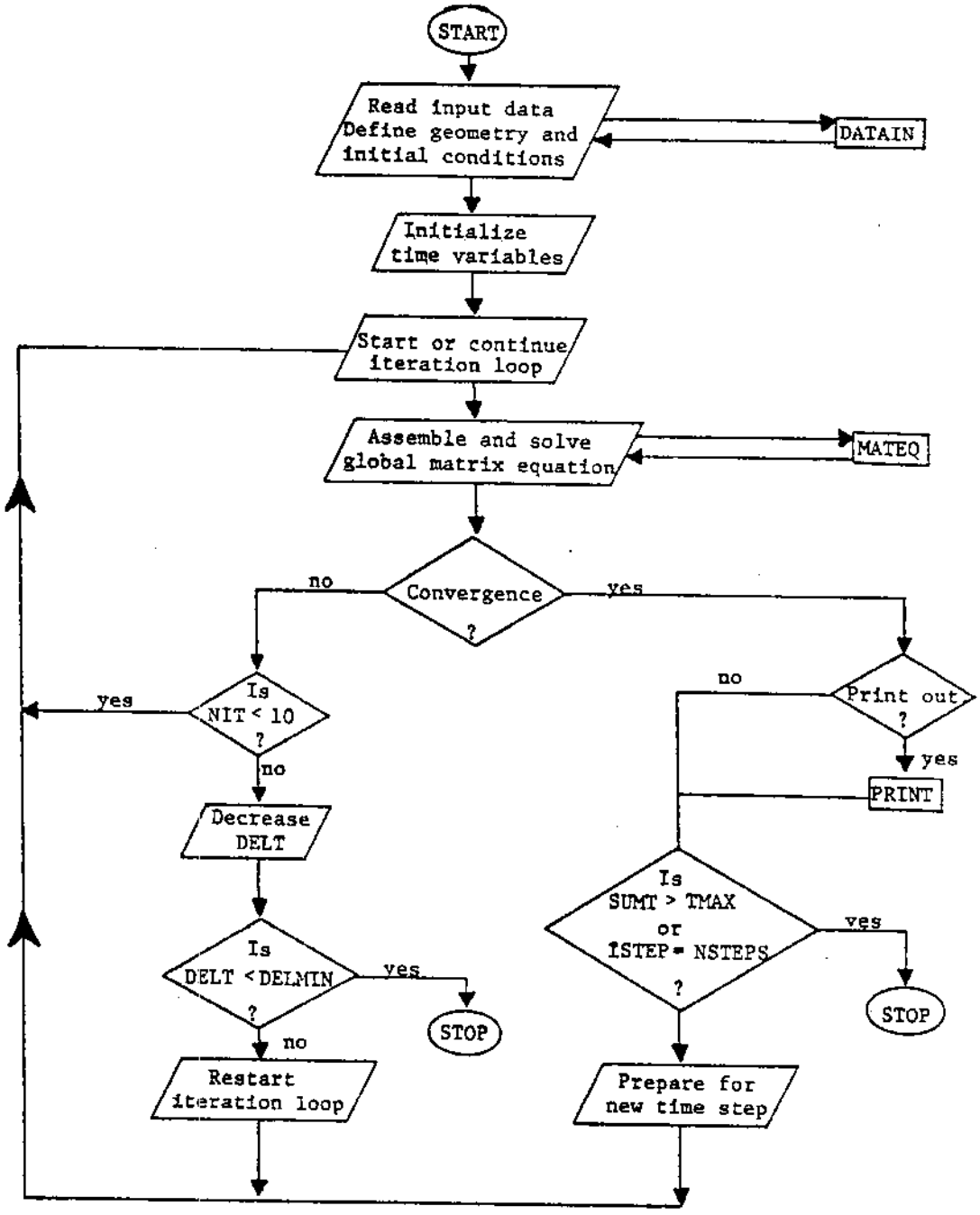

Fig. A1. Generalized flow chart of UNSAT1.

present version these functions are given by means of analytical expressions. If necessary, they can, of course, also be given in table form.

Table A1 gives a listing of the most significant variables in UNSAT1. Instructions for preparing the data cards are given in Table A2, while Table A3 specifies the actual data cards used for example 2. Part of the computer output for this example is given in Table A4, while the actual listing of the program is given in Table A5.

Table A1. Definition of the main program variables of UNSAT1. If the variable appears in only one function or subroutine, the name of that function of subroutine is given after the definition. If the variable represents an array, the maximum dimension of that array is also specified.

VARIABLE	*DEFINITION*
A(5)	Vector used to calculate the moisture contents of each soil type for possible print-out (DATAIN).
ALPHA(NMAT)	Values of the coefficients α for each soil type (SPR).
B(5)	Vector used to calculate the hydraulic conductivities of each soil type for possible print-out (DATAIN).
BC(K,SUMT)	Subroutine used to define the transient boundary condition at the soil surface. If K=1, the subroutine gives a first-type (given pressure) boundary condition as a function of time (SUMT); if K=2, a second-type (flux) boundary condition is given as a function of time.
CAP1, CAP2, CAP3	Functions of the soil moisture capacity at the nodal interior Lobatto integration points (MATEQ).
COND1, COND2, COND3	Functions of the hydraulic conductivity at the nodal or interior Lobatto integration points (MATEQ).
CONDM	Minimum value of the unsaturated hydraulic conductivity (SPR).
CONSM(NMAT)	Values of the saturated hydraulic conductivity for each soil type (SPR).
DELCH	Change in DELT between two consecutive time steps (MAIN).
DELMAX	Maximum value of DELT during execution.
DELMIN	Minimum value of DELT permitted during execution.
DELT	Time increment.
DRAIN	Drainage rate.
DX(4,3)	Derivatives of the four basis functions, evaluated at the three interior Lobatto integration points (MATEQ).
EL	Nodal distance.
EPSI	Weighting coefficient.
EPSM	= EPSI -1 (MATEQ).

Table A1. (continued):

VARIABLE	*DEFINITION*
F(NEQ)	Right-hand side vector of global matrix equation (MATEQ).
FE(4,3)	Values of the four basis functions, evaluated at the three interior Lobatto integration points (MATEQ).
INT(NN)	Array indicating type of material interpolation between two consecutive nodes. If INT=1, the soil properties are assumed to change linearly; if INT=0, a restricted Hermitian interpolation is used.
ISPR(NN)	Soil property index, defining soil type for each node.
ISTEP	Number of times steps since start of simulation (MAIN).
KDRAIN	Drainage code for lower boundary: =0 if the pressure head is specified. =1 if the pressure gradient is specified. =2 if the drainage rate (DRAIN) is specified. =3 if both the pressure head and its gradient are specified.
KOD1	Output code. If KOD1=1, the solution vector is printed after each iteration. If KOD1=0, no such output is given.
KOD2	Input code. If KOD2=0, initial moisture contents are read in and converted to pressure heads. If KOD2=1, pressure head values are read in (DATAIN).
KOD3	Output code. If KOD3=N (N≤NMAT), the soil-hydraulic properties of the first N soil-types are printed. If KOD3=0, no such output is given (DATAIN).
KRAIN	Rainfall code for soil surface boundary: =0 if the pressure head is specified. =1 if the infiltration rate (RAIN) is specified.
L	Element number.
MAT, MAT1, MAT2	Material index of certain node or integration point.
N1	=NN2-1.
N2	=NN2-2.
N3	=NN2-3.
NE	Number of elements (=NN-1).

Table A1. (continued):

VARIABLE	*DEFINITION*
NEQ	Number of equations to be solved (MATEQ): =N1 if KDRAIN=0, 1 or 2, =N2 if KDRAIN=3.
NIT	Number of iterations during particular time step (MAIN).
NITMAX	Maximum number of iterations (set to 10)(MAIN).
NITT	Total number of iterations since start of simulation.
NMAT	Number of different soil types (dummy variable).
NN	Number of nodes.
NN2	=2*NN.
NSTEPS	Maximum number of time steps permitted.
P(NN2)	Vector of pressure heads and gradients at old time level.
PE(NN2)	Estimated or calculated vector of pressure heads and gradients for new time level.
PRDEL	Time increment for printed output.
PRTIME	Dummy variable, used to calculate output for every PRDEL (MAIN).
PULSE	Irreversible time switch for changing from a first-type to a flux-type boundary condition.
R0(I)	Data points for transient first-type boundary condition (BC).
R1(I)	Data points for transient flux-type boundary condition (BC).
RAIN	Transient precipitation or evaporation rate.
RN(MAT)	Values of the exponent n in the soil moisture retention curve for each soil type (SPR).
S(NN2,4)	Global coefficient matrix (MATEQ).
SPR(MAT,N,P)	Function to calculate the soil hydraulic properties of material MAT: if N=1, the soil moisture content is given as a function of the pressure head P. if N=2, the hydraulic conductivity is given as a function of the pressure head P.

Table A1. (continued):

VARIABLE	*DEFINITION*
	if N=3, the soil moisture capacity is given as a function of the pressure head P. if N=4, the pressure head is given as a function of the soil moisture content.
SR(10)	Vector containing contributions of the three interior integration points to the right-hand side vector of each element matrix equation (MATEQ).
SUMT1, SUMT2, SUMT3	Elapsed time since start of simulation, in hours, minutes, and seconds, respectively (PRINT).
T(NN2)	Temporary storage vector for pressure heads and gradients during iterative solution process (MAIN).
TO(I)	Vector used to specify the transient first-type boundary condition in table form (BC).
T1(I)	Vector used to specify the transient flux-type boundary condition in table form (BC).
THETA	Dimensionless moisture content (SPR).
TITLE(20)	Array containing information of program title cards (DATAIN).
TMAX	Maximum simulation time.
TMDIFF	Error in the material balance calculations: TMDIFF=TMINF-TMINCR (PRINT).
TMIN	Total amount of moisture in soil profile.
TMINCR	Increase in stored moisture since start of simulation: TMINCR=TMIN-TMINIT.
TMINF	Cumulative uptake of moisture by profile since start of simulation, i.e., cumulative infiltration minus cumulative drainage.
TMINIT	Total amount of moisture in soil profile at start of simulation.
TOL	Convergence criterion for iterative solution process.
TOL1	Absolute convergence criterion.
TOL2	Relative convergence criterion.

Table A1. (continued):

VARIABLE	*DEFINITION*
WC	Variable generally defining the soil moisture content.
WCR(NMAT)	Residual moisture content for each soil type (SPR).
WCS(NMAT)	Saturated moisture content for each soil type (SPR).
X(NN)	Nodal coordinates.

Table A2. Input data instructions for UNSAT1.

CARDS	*COLUMNS*	*FORMAT*	*VARIABLE*	*COMMENT*
1,2,3	1-80	20(A4)	TITLE	
4	1-5	I5	NN	Number of nodes.
	6-10	I5	NSTEPS	Maximum number of time steps.
	11-20	F10.0	DELT	Initial time step (days).
	21-30	F10.0	DELMIN	Minimum permitted time step (days).
	31-40	F10.0	DELMAX	Maximum time step (days).
	41-50	F10.0	TMAX	Maximum simulation time (days).
	51-60	F10.0	PRDEL	Time step for print-out (days).
	61-70	F10.0	PULSE	Time switch for soil surface. boundary condition (days).
	71-80	F10.0	EPSI	Weighting coefficient.
5	1-5	I5	KRAIN	Rainfall code.
	6-10	I5	KDRAIN	Drainage code.
	11-15	I5	KOD1	Output code.
	16-20	I5	KOD2	Input code.
	21-25	I5	KOD3	Output code.
	26-35	F10.0	DRAIN	Drainage rate (cm/day).
	36-45	F10.0	TOL1	Absolute convergence criterion (cm).
	46-55	F10.0	TOL2	Relative convergence criterion.
6,etc.	1-5	I5	I	Nodal number.
	6-10	I5	ISPR(I)	Soil property index of node I.
	11-20	F10.0	X(I)	Coordinate of node I (cm).
	21-30	F10.0	P(2I-1)	Initial pressure head if KOD2=1, initial moisture content if KOD2=0.
	31-40	F10.0	P(2I)	Initial pressure gradient if KOD2=1, initial moisture gradient if KOD2=0.
	41-45	15	INT(I)	Interpolation index for element I.

Table A3. Data input for example 2.

```
      UNSAT1                                                    EXAMPLE 2

      NOVEMBER, 1978                                            HERMITE (SLP)
27 5000  .0005     .00005       0.5          8.0        .050          0.50          0.50
 1    1     0    1     9      0.0      0.50      0.005
 1    1    0.0          -350.0          0.0
 2    1    6.0          -350.0          0.0
 3    1   14.0          -350.0          0.0
 4    1   22.0          -350.0          0.0
 5    3   28.0          -350.0          0.0       1
 6    4   36.0          -350.0          0.0       1
 7    5   46.0          -350.0          0.0       1
 8    6   55.0          -350.0          0.0       1
 9    7   63.0          -350.0          0.0       1
10    8   69.0          -350.0          0.0       1
11    9   73.0          -350.0          0.0
12    2   77.0          -350.0          0.0
13    2   81.0          -350.0          0.0
14    2   85.0          -350.0          0.0
15    9   89.0          -350.0          0.0
16    9   93.0          -350.0          0.0
17    9   97.0          -350.0          0.0
18    9  102.0          -350.0          0.0
19    9  107.0          -350.0          0.0
20    9  112.0          -350.0          0.0
21    9  118.0          -350.0          0.0
22    9  125.0          -350.0          0.0
23    9  133.0          -350.0          0.0
24    9  141.0          -350.0          0.0
25    9  150.0          -350.0          0.0
26    9  160.0          -350.0          0.0
27    9  170.0          -350.0          0.0
```

Table A4. Partial output for example 2.

```
*******************************************************************************
*                                                                             *
*          ONE-DIMENSIONAL SATURATED-UNSATURATED FLOW                         *
*                                                                             *
*          UNSAT1                                  EXAMPLE 2                  *
*                                                                             *
*          NOVEMBER, 1978                          HERMITE (5LP)              *
*                                                                             *
*******************************************************************************
```

INPUT PARAMETERS

NUMBER OF NODES	(NN)	27
MAXIMUM NUMBER OF TIME STEPS	(NSTEPS)	5000
INITIAL TIME STEP	(DELT)	0.50000E-03
MINIMUM ALLOWABLE TIME STEP	(DELMIN)	0.50000E-04
MAXIMUM ALLOWABLE TIME STEP	(DELMAX)	0.50000E 00
MAXIMUM SIMULATION TIME	(TMAX)	8.000
PRINT DELT FOR OUTPUT	(PRDEL)	0.050
PULSE LENGTH FOR 1ST-TYPE BC	(PULSE)	0.500
WEIGHTING COEFFICIENT	(EPSI)	0.500

REDEFINED SURFACE VALUES

ITERATION	MOIST. CONT.	PRESSURE	GRADIENT
1	0.3946	-208.337	-67.8547
2	0.3854	-226.467	-88.6986
3	0.3842	-228.800	-91.7099
4	0.3842	-228.989	-91.9566

ADDITIONAL PARAMETERS

ITERATION TOLERANCE	(TOL1)	0.500
ITERATION TOLERANCE	(TOL2)	0.005
INITIAL INFILTRATION RATE	(RAIN)	25.000
INITIAL DRAINAGE RATE	(DRAIN)	0.008
KRAIN	(RAINFALL CODE)	1
KDRAIN	(DRAINAGE CODE)	1
KOD1	(OUTPUT FOR EVERY ITERATION)	0
KOD2	(INPUT VARIABLE IS PRESSURE HEAD)	1
KOD3	(WRITE MATERIAL PROPERTIES)	9

INITIAL CONDITIONS

		PRESSURE HEAD				MOISTURE CONTENT				INDICES	
NODE	DEPTH	FUNCTION	GRADIENT	F(-1/3)	F(+1/3)	FUNCTN	GRADNT	F(-1/3)	F(+1/3)	MAT	INT
1	0.0	-228.989	-91.957	-342.101	-359.496	0.3842	-0.0443	0.3421	0.3373	1	0
2	6.00	-350.000	0.0	-350.000	-350.000	0.3398	0.0	0.3398	0.3398	1	0
3	14.00	-350.000	0.0	-350.000	-350.000	0.3398	0.0	0.3398	0.3398	1	0
4	22.00	-350.000	0.0	-350.000	-350.000	0.3398	0.0	0.3172	0.2751	1	0
5	28.00	-350.000	0.0	-350.000	-350.000	0.2524	0.0	0.2432	0.2340	3	1
6	36.00	-350.000	0.0	-350.000	-350.000	0.2248	0.0	0.2151	0.2053	4	1
7	46.00	-350.000	0.0	-350.000	-350.000	0.1955	0.0	0.1881	0.1806	5	1
8	55.00	-350.000	0.0	-350.000	-350.000	0.1731	0.0	0.1673	0.1616	6	1
9	63.00	-350.000	0.0	-350.000	-350.000	0.1558	0.0	0.1519	0.1480	7	1
10	69.00	-350.000	0.0	-350.000	-350.000	0.1441	0.0	0.1417	0.1393	8	1
11	73.00	-350.000	0.0	-350.000	-350.000	0.1369	0.0	0.1700	0.2316	9	0
12	77.00	-350.000	0.0	-350.000	-350.000	0.2648	0.0	0.2648	0.2648	2	0
13	81.00	-350.000	0.0	-350.000	-350.000	0.2648	0.0	0.2648	0.2648	2	0
14	85.00	-350.000	0.0	-350.000	-350.000	0.2648	0.0	0.2316	0.1700	2	0
15	89.00	-350.000	0.0	-350.000	-350.000	0.1369	0.0	0.1369	0.1369	9	0
16	93.00	-350.000	0.0	-350.000	-350.000	0.1369	0.0	0.1369	0.1369	9	0
17	97.00	-350.000	0.0	-350.000	-350.000	0.1369	0.0	0.1369	0.1369	9	0
18	102.00	-350.000	0.0	-350.000	-350.000	0.1369	0.0	0.1369	0.1369	9	0
19	107.00	-350.000	0.0	-350.000	-350.000	0.1369	0.0	0.1369	0.1369	9	0
20	112.00	-350.000	0.0	-350.000	-350.000	0.1369	0.0	0.1369	0.1369	9	0
21	118.00	-350.000	0.0	-350.000	-350.000	0.1369	0.0	0.1369	0.1369	9	0
22	125.00	-350.000	0.0	-350.000	-350.000	0.1369	0.0	0.1369	0.1369	9	0
23	133.00	-350.000	0.0	-350.000	-350.000	0.1369	0.0	0.1369	0.1369	9	0
24	141.00	-350.000	0.0	-350.000	-350.000	0.1369	0.0	0.1369	0.1369	9	0
25	150.00	-350.000	0.0	-350.000	-350.000	0.1369	0.0	0.1369	0.1369	9	0
26	160.00	-350.000	0.0	-350.000	-350.000	0.1369	0.0	0.1369	0.1369	9	0
27	170.00	-350.000	0.0			0.1369	0.0			9	

INITIAL AMOUNT OF MOISTURE IN PROFILE: 32.5541 CM3

SOIL-HYDRAULIC PROPERTIES (MOISTURE CONTENT AND HYDRAULIC CONDUCTIVITY)

PRESSURE HEAD	SOIL 1 WC	SOIL 1 COND	SOIL 2 WC	SOIL 2 COND	SOIL 3 WC	SOIL 3 COND	SOIL 4 WC	SOIL 4 COND	SOIL 5 WC	SOIL 5 COND
-0.600E 00	0.5400	0.243E 02	0.4000	0.100E 02	0.4700	0.741E 02	0.4611	0.132E 03	0.4500	0.205E 03
-0.720E 00	0.5400	0.242E 02	0.4000	0.100E 02	0.4700	0.739E 02	0.4611	0.132E 03	0.4500	0.205E 03
-0.864E 00	0.5400	0.241E 02	0.4000	0.100E 02	0.4700	0.737E 02	0.4611	0.132E 03	0.4500	0.204E 03
-0.104E 01	0.5400	0.239E 02	0.4000	0.100E 02	0.4700	0.735E 02	0.4611	0.132E 03	0.4500	0.204E 03
-0.124E 01	0.5400	0.238E 02	0.4000	0.100E 02	0.4700	0.731E 02	0.4611	0.131E 03	0.4500	0.204E 03
-0.149E 01	0.5399	0.236E 02	0.4000	0.100E 02	0.4700	0.728E 02	0.4611	0.131E 03	0.4500	0.204E 03
-0.179E 01	0.5399	0.234E 02	0.4000	0.999E 01	0.4700	0.723E 02	0.4611	0.130E 03	0.4500	0.203E 03
-0.215E 01	0.5399	0.231E 02	0.4000	0.999E 01	0.4699	0.716E 02	0.4611	0.130E 03	0.4500	0.203E 03
-0.258E 01	0.5399	0.228E 02	0.4000	0.999E 01	0.4699	0.712E 02	0.4610	0.129E 03	0.4500	0.202E 03
-0.310E 01	0.5398	0.225E 02	0.4000	0.998E 01	0.4699	0.704E 02	0.4610	0.128E 03	0.4499	0.201E 03
-0.372E 01	0.5397	0.221E 02	0.4000	0.998E 01	0.4698	0.695E 02	0.4610	0.127E 03	0.4499	0.200E 03
-0.446E 01	0.5396	0.216E 02	0.4000	0.997E 01	0.4697	0.684E 02	0.4609	0.126E 03	0.4499	0.199E 03
-0.535E 01	0.5395	0.211E 02	0.4000	0.995E 01	0.4696	0.672E 02	0.4608	0.124E 03	0.4498	0.197E 03
-0.642E 01	0.5393	0.206E 02	0.4000	0.993E 01	0.4694	0.656E 02	0.4607	0.122E 03	0.4497	0.195E 03
-0.770E 01	0.5390	0.199E 02	0.4000	0.990E 01	0.4691	0.638E 02	0.4604	0.120E 03	0.4496	0.192E 03
-0.924E 01	0.5386	0.191E 02	0.3999	0.986E 01	0.4687	0.617E 02	0.4601	0.116E 03	0.4493	0.189E 03
-0.111E 02	0.5381	0.183E 02	0.3999	0.980E 01	0.4682	0.592E 02	0.4597	0.113E 03	0.4489	0.184E 03
-0.133E 02	0.5374	0.173E 02	0.3998	0.971E 01	0.4674	0.563E 02	0.4590	0.108E 03	0.4483	0.178E 03
-0.160E 02	0.5363	0.163E 02	0.3997	0.958E 01	0.4662	0.529E 02	0.4579	0.103E 03	0.4475	0.171E 03
-0.192E 02	0.5350	0.151E 02	0.3995	0.940E 01	0.4646	0.490E 02	0.4564	0.960E 02	0.4461	0.162E 03
-0.230E 02	0.5331	0.138E 02	0.3991	0.914E 01	0.4624	0.446E 02	0.4542	0.882E 02	0.4440	0.150E 03
-0.276E 02	0.5305	0.124E 02	0.3985	0.877E 01	0.4592	0.397E 02	0.4510	0.792E 02	0.4408	0.136E 03
-0.331E 02	0.5270	0.109E 02	0.3974	0.826E 01	0.4548	0.343E 02	0.4464	0.691E 02	0.4361	0.120E 03
-0.397E 02	0.5224	0.938E 01	0.3956	0.756E 01	0.4488	0.288E 02	0.4399	0.580E 02	0.4292	0.101E 03
-0.477E 02	0.5163	0.782E 01	0.3926	0.663E 01	0.4408	0.231E 02	0.4311	0.465E 02	0.4193	0.809E 02
-0.572E 02	0.5084	0.630E 01	0.3877	0.548E 01	0.4304	0.177E 02	0.4192	0.353E 02	0.4057	0.605E 02
-0.687E 02	0.4985	0.488E 01	0.3802	0.416E 01	0.4173	0.128E 02	0.4041	0.250E 02	0.3879	0.417E 02
-0.824E 02	0.4863	0.361E 01	0.3694	0.282E 01	0.4015	0.873E 01	0.3856	0.165E 02	0.3660	0.262E 02
-0.989E 02	0.4717	0.254E 01	0.3551	0.166E 01	0.3833	0.557E 01	0.3643	0.100E 02	0.3408	0.149E 02
-0.119E 03	0.4550	0.170E 01	0.3382	0.831E 00	0.3633	0.333E 01	0.3412	0.564E 01	0.3140	0.774E 01
-0.142E 03	0.4364	0.108E 01	0.3205	0.357E 00	0.3424	0.187E 01	0.3175	0.295E 01	0.2875	0.367E 01
-0.171E 03	0.4167	0.658E 00	0.3039	0.134E 00	0.3215	0.999E 00	0.2946	0.145E 01	0.2627	0.162E 01
-0.205E 03	0.3964	0.381E 00	0.2899	0.453E-01	0.3015	0.508E 00	0.2733	0.677E 00	0.2409	0.678E 00
-0.246E 03	0.3763	0.213E 00	0.2788	0.142E-01	0.2829	0.249E 00	0.2543	0.304E 00	0.2224	0.272E 00
-0.295E 03	0.3569	0.115E 00	0.2705	0.427E-02	0.2662	0.119E 00	0.2379	0.132E 00	0.2071	0.106E 00
-0.354E 03	0.3386	0.602E-01	0.2644	0.125E-02	0.2515	0.552E-01	0.2239	0.564E-01	0.1948	0.403E-01
-0.425E 03	0.3219	0.309E-01	0.2601	0.356E-03	0.2387	0.253E-01	0.2123	0.237E-01	0.1850	0.152E-01
-0.510E 03	0.3067	0.156E-01	0.2571	0.101E-03	0.2277	0.115E-01	0.2027	0.983E-02	0.1772	0.566E-02
-0.612E 03	0.2930	0.781E-02	0.2549	0.284E-04	0.2183	0.514E-02	0.1948	0.405E-02	0.1712	0.210E-02
-0.735E 03	0.2810	0.386E-02	0.2534	0.796E-05	0.2105	0.230E-02	0.1884	0.166E-02	0.1664	0.776E-03
-0.882E 03	0.2703	0.190E-02	0.2524	0.223E-05	0.2038	0.102E-02	0.1832	0.680E-03	0.1628	0.286E-03
-0.106E 04	0.2610	0.928E-03	0.2517	0.624E-06	0.1982	0.452E-03	0.1789	0.277E-03	0.1599	0.105E-03
-0.127E 04	0.2529	0.452E-03	0.2511	0.174E-06	0.1936	0.200E-03	0.1755	0.113E-03	0.1577	0.367E-04
-0.152E 04	0.2458	0.219E-03	0.2508	0.487E-07	0.1896	0.884E-04	0.1727	0.459E-04	0.1559	0.142E-04
-0.183E 04	0.2396	0.106E-03	0.2506	0.136E-07	0.1864	0.390E-04	0.1705	0.186E-04	0.1546	0.522E-05
-0.219E 04	0.2343	0.515E-04	0.2504	0.100E-07	0.1837	0.172E-04	0.1687	0.758E-05	0.1536	0.191E-05
-0.263E 04	0.2296	0.249E-04	0.2503	0.100E-07	0.1814	0.758E-05	0.1672	0.308E-05	0.1528	0.703E-06

-0.316E 04	0.2256	0.120E-04	0.2502	0.100E-07	0.1795	0.334E-05	0.1660	0.125E-05	0.1521	0.258E-06
-0.379E 04	0.2222	0.581E-05	0.2501	0.100E-07	0.1779	0.147E-05	0.1651	0.508E-06	0.1517	0.946E-07
-0.455E 04	0.2192	0.281E-05	0.2501	0.100E-07	0.1766	0.648E-06	0.1643	0.206E-06	0.1513	0.347E-07
-0.546E 04	0.2166	0.135E-05	0.2501	0.100E-07	0.1755	0.285E-06	0.1637	0.837E-07	0.1510	0.127E-07
-0.655E 04	0.2143	0.653E-06	0.2500	0.100E-07	0.1746	0.126E-06	0.1632	0.340E-07	0.1508	0.100E-07
-0.786E 04	0.2124	0.315E-06	0.2500	0.100E-07	0.1738	0.553E-07	0.1628	0.138E-07	0.1506	0.100E-07
-0.944E 04	0.2107	0.152E-06	0.2500	0.100E-07	0.1732	0.244E-07	0.1625	0.100E-07	0.1505	0.100E-07

SOIL-HYDRAULIC PROPERTIES (MOISTURE CONTENT AND HYDRAULIC CONDUCTIVITY)

PRESSURE HEAD	SOIL 6		SOIL 7		SOIL 8		SOIL 9		SOIL 10	
	WC	COND	WC	COND	WC	COND	WC	COND	WC	COND
-0.600E 00	0.4400	0.270E 03	0.4311	0.328E 03	0.4244	0.371E 03	0.4200	0.400E 03		
-0.720E 00	0.4400	0.270E 03	0.4311	0.328E 03	0.4244	0.371E 03	0.4200	0.400E 03		
-0.864E 00	0.4400	0.270E 03	0.4311	0.328E 03	0.4244	0.371E 03	0.4200	0.400E 03		
-0.104E 01	0.4400	0.270E 03	0.4311	0.328E 03	0.4244	0.371E 03	0.4200	0.400E 03		
-0.124E 01	0.4400	0.269E 03	0.4311	0.327E 03	0.4244	0.371E 03	0.4200	0.400E 03		
-0.149E 01	0.4400	0.269E 03	0.4311	0.327E 03	0.4244	0.371E 03	0.4200	0.400E 03		
-0.179E 01	0.4400	0.269E 03	0.4311	0.327E 03	0.4244	0.371E 03	0.4200	0.400E 03		
-0.215E 01	0.4400	0.269E 03	0.4311	0.327E 03	0.4244	0.370E 03	0.4200	0.399E 03		
-0.258E 01	0.4400	0.268E 03	0.4311	0.327E 03	0.4244	0.370E 03	0.4200	0.399E 03		
-0.310E 01	0.4400	0.268E 03	0.4311	0.326E 03	0.4244	0.370E 03	0.4200	0.399E 03		
-0.372E 01	0.4400	0.267E 03	0.4311	0.325E 03	0.4244	0.369E 03	0.4200	0.398E 03		
-0.446E 01	0.4399	0.266E 03	0.4310	0.324E 03	0.4244	0.368E 03	0.4200	0.396E 03		
-0.535E 01	0.4399	0.264E 03	0.4310	0.323E 03	0.4243	0.367E 03	0.4199	0.397E 03		
-0.642E 01	0.4398	0.262E 03	0.4310	0.321E 03	0.4243	0.366E 03	0.4199	0.395E 03		
-0.770E 01	0.4397	0.259E 03	0.4309	0.319E 03	0.4242	0.363E 03	0.4198	0.393E 03		
-0.924E 01	0.4395	0.256E 03	0.4307	0.315E 03	0.4241	0.360E 03	0.4197	0.390E 03		
-0.111E 02	0.4392	0.251E 03	0.4305	0.311E 03	0.4239	0.356E 03	0.4195	0.386E 03		
-0.133E 02	0.4387	0.244E 03	0.4300	0.304E 03	0.4235	0.349E 03	0.4192	0.379E 03		
-0.160E 02	0.4379	0.236E 03	0.4294	0.295E 03	0.4229	0.340E 03	0.4186	0.370E 03		
-0.192E 02	0.4367	0.225E 03	0.4282	0.283E 03	0.4218	0.328E 03	0.4176	0.358E 03		
-0.230E 02	0.4347	0.211E 03	0.4264	0.267E 03	0.4200	0.311E 03	0.4159	0.340E 03		
-0.276E 02	0.4316	0.193E 03	0.4233	0.246E 03	0.4171	0.287E 03	0.4129	0.315E 03		
-0.331E 02	0.4268	0.171E 03	0.4185	0.219E 03	0.4122	0.257E 03	0.4061	0.282E 03		
-0.397E 02	0.4195	0.145E 03	0.4109	0.186E 03	0.4044	0.218E 03	0.4001	0.240E 03		
-0.477E 02	0.4087	0.115E 03	0.3993	0.147E 03	0.3922	0.172E 03	0.3875	0.189E 03		
-0.572E 02	0.3935	0.850E 02	0.3826	0.107E 03	0.3743	0.124E 03	0.3668	0.135E 03		
-0.687E 02	0.3732	0.569E 02	0.3599	0.698E 02	0.3499	0.789E 02	0.3430	0.845E 02		
-0.824E 02	0.3481	0.342E 02	0.3318	0.400E 02	0.3194	0.436E 02	0.3111	0.454E 02		
-0.989E 02	0.3195	0.182E 02	0.3001	0.200E 02	0.2856	0.207E 02	0.2758	0.208E 02		
-0.119E 03	0.2897	0.868E 01	0.2680	0.880E 01	0.2520	0.855E 01	0.2413	0.822E 01		
-0.142E 03	0.2611	0.375E 01	0.2383	0.348E 01	0.2217	0.315E 01	0.2109	0.289E 01		
-0.171E 03	0.2356	0.150E 01	0.2128	0.126E 01	0.1967	0.107E 01	0.1863	0.935E 00		
-0.205E 03	0.2142	0.564E 00	0.1922	0.434E 00	0.1770	0.342E 00	0.1674	0.285E 00		
-0.246E 03	0.1968	0.204E 00	0.1763	0.143E 00	0.1623	0.105E 00	0.1535	0.841E-01		
-0.295E 03	0.1831	0.718E-01	0.1642	0.461E-01	0.1515	0.318E-01	0.1435	0.242E-01		
-0.354E 03	0.1725	0.248E-01	0.1552	0.146E-01	0.1436	0.943E-02	0.1364	0.689E-02		
-0.425E 03	0.1644	0.847E-02	0.1486	0.457E-02	0.1380	0.277E-02	0.1315	0.194E-02		
-0.510E 03	0.1583	0.287E-02	0.1438	0.143E-02	0.1340	0.811E-03	0.1280	0.545E-03		
-0.612E 03	0.1537	0.970E-03	0.1403	0.442E-03	0.1312	0.237E-03	0.1255	0.153E-03		
-0.735E 03	0.1503	0.326E-03	0.1378	0.137E-03	0.1292	0.690E-04	0.1239	0.427E-04		
-0.882E 03	0.1477	0.109E-03	0.1359	0.424E-04	0.1278	0.201E-04	0.1227	0.119E-04		
-0.106E 04	0.1457	0.368E-04	0.1346	0.131E-04	0.1268	0.585E-05	0.1219	0.353E-05		
-0.127E 04	0.1443	0.123E-04	0.1336	0.405E-05	0.1261	0.170E-05	0.1213	0.931E-06		
-0.152E 04	0.1432	0.413E-05	0.1329	0.125E-05	0.1256	0.495E-06	0.1209	0.260E-06		
-0.183E 04	0.1424	0.138E-05	0.1324	0.387E-06	0.1252	0.144E-06	0.1206	0.726E-07		
-0.219E 04	0.1418	0.464E-06	0.1321	0.120E-06	0.1250	0.418E-07	0.1204	0.203E-07		
-0.263E 04	0.1413	0.155E-06	0.1318	0.369E-07	0.1248	0.121E-07	0.1203	0.100E-07		

-0.316E 04	0.1410	0.520E-07	0.1316	0.114E-07	0.1247	0.100E-07	0.1202	0.100E-07
-0.379E 04	0.1407	0.174E-07	0.1315	0.100E-07	0.1246	0.100E-07	0.1201	0.100E-07
-0.455E 04	0.1406	0.100E-07	0.1314	0.100E-07	0.1245	0.100E-07	0.1201	0.100E-07
-0.546E 04	0.1404	0.100E-07	0.1313	0.100E-07	0.1245	0.100E-07	0.1201	0.100E-07
-0.655E 04	0.1403	0.100E-07	0.1312	0.100E-07	0.1245	0.100E-07	0.1200	0.100E-07
-0.786E 04	0.1402	0.100E-07	0.1312	0.100E-07	0.1245	0.100E-07	0.1200	0.100E-07
-0.944E 04	0.1402	0.100E-07	0.1312	0.100E-07	0.1244	0.100E-07	0.1200	0.100E-07

ELAPSED TIME	DAYS	HOURS	MINUTES	SECONDS	TIME STEP	STEP #	NIT	NITT
	0.0513	1.231	0.7384E 02	0.4430E 04	0.58208E-02	21	3	48

		PRESSURE HEAD				MOISTURE CONTENT			
NODE	DEPTH	FUNCTION	GRADIENT	F(-1/3)	F(+1/3)	FUNCTN	GRADNT	F(-1/3)	F(+1/3)
1	0.0	-77.480	-5.205	-89.435	-104.694	0.4907	-0.0046	0.4800	0.4667
2	6.00	-123.576	-10.400	-165.928	-230.349	0.4510	-0.0084	0.4199	0.3835
3	14.00	-306.084	-29.178	-349.355	-350.026	0.3532	-0.0097	0.3400	0.3398
4	22.00	-347.801	-3.586	-351.162	-350.101	0.3405	-0.0010	0.3169	0.2751
5	28.00	-349.416	-0.550	-350.134	-349.940	0.2525	-0.0001	0.2432	0.2340
6	36.00	-349.705	-0.012	-349.661	-349.536	0.2249	-0.0000	0.2151	0.2054
7	46.00	-349.467	-0.001	-349.444	-349.412	0.1956	-0.0000	0.1862	0.1807
8	55.00	-349.432	-0.022	-349.461	-349.469	0.1732	-0.0000	0.1674	0.1616
9	63.00	-349.511	-0.029	-349.550	-349.567	0.1558	-0.0000	0.1519	0.1480
10	69.00	-349.581	-0.010	-349.583	-349.536	0.1441	-0.0000	0.1417	0.1393
11	73.00	-349.403	0.142	-349.179	-349.112	0.1369	0.0000	0.1701	0.2317
12	77.00	-349.545	-0.596	-349.976	-349.976	0.2648	-0.0000	0.2648	0.2648
13	81.00	-349.984	-0.118	-349.991	-349.989	0.2648	-0.0000	0.2648	0.2648
14	85.00	-350.409	-0.581	-350.818	-350.706	0.2648	-0.0000	0.2316	0.1700
15	89.00	-350.590	0.236	-350.157	-350.050	0.1368	0.0000	0.1368	0.1369
16	93.00	-350.009	0.020	-349.991	-349.986	0.1369	0.0000	0.1369	0.1369
17	97.00	-349.987	0.000	-349.986	-349.984	0.1369	0.0000	0.1369	0.1369
18	102.00	-349.984	-0.000	-349.984	-349.984	0.1369	-0.0000	0.1369	0.1369
19	107.00	-349.985	-0.001	-349.985	-349.984	0.1369	-0.0000	0.1369	0.1369
20	112.00	-349.985	-0.001	-349.985	-349.985	0.1369	-0.0000	0.1369	0.1369
21	118.00	-349.987	-0.002	-349.987	-349.985	0.1369	-0.0000	0.1369	0.1369
22	125.00	-349.986	-0.002	-349.988	-349.986	0.1369	-0.0000	0.1369	0.1369
23	133.00	-349.987	-0.001	-349.987	-349.985	0.1369	-0.0000	0.1369	0.1369
24	141.00	-349.987	-0.002	-349.987	-349.984	0.1369	-0.0000	0.1369	0.1369
25	150.00	-349.984	-0.002	-349.987	-349.987	0.1369	-0.0000	0.1369	0.1369
26	160.00	-349.987	-0.001	-349.990	-349.992	0.1369	-0.0000	0.1369	0.1369
27	170.00	-349.994	0.0			0.1369	0.0		

INFILTRATION RATE(CM/DAY).....	25.000
DRAINAGE RATE(CM/DAY).....	0.008
TOTAL MOISTURE IN PROFILE(CM3)...	33.825
MOISTURE ADDED TO PROFILE (CM3).....	1.281
MOISTURE INCREASE IN PROFILE(CM3)....	1.271
DEVIATION(CM3).....	0.011

ELAPSED TIME	DAYS	HOURS	MINUTES	SECONDS	TIME STEP	STEP #	NIT	NITT
	0.0971	2.331	0.1396E 03	0.8391E 04	0.90949E-02	27	2	63

		PRESSURE HEAD				MOISTURE CONTENT			
NODE	DEPTH	FUNCTION	GRADIENT	F(-1/3)	F(+1/3)	FUNCTN	GRADNT	F(-1/3)	F(+1/3)
1	0.0	-55.677	-2.856	-61.912	-69.258	0.5098	-0.0024	0.5044	0.4980
2	6.00	-77.810	-4.594	-92.146	-111.675	0.4904	-0.0041	0.4776	0.4606
3	14.00	-137.933	-11.300	-160.851	-241.688	0.4398	-0.0086	0.4104	0.3782
4	22.00	-308.960	-24.999	-340.382	-347.065	0.3522	-0.0082	0.3197	0.2758
5	28.00	-347.630	-1.855	-350.177	-349.806	0.2529	-0.0004	0.2432	0.2341

6	36.00	-349.336	-0.157	-349.465	-349.172	0.2250	-0.0000	0.2152	0.2055
7	46.00	-349.008	-0.025	-348.999	-348.924	0.1957	-0.0000	0.1882	0.1808
8	55.00	-348.935	-0.035	-348.987	-349.008	0.1733	-0.0000	0.1675	0.1617
9	63.00	-349.074	-0.042	-349.136	-349.164	0.1559	-0.0000	0.1520	0.1481
10	69.00	-349.169	0.001	-349.145	-349.057	0.1442	0.0000	0.1416	0.1394
11	73.00	-348.878	0.176	-348.600	-348.538	0.1370	0.0000	0.1702	0.2318
12	77.00	-349.145	-0.819	-349.818	-349.950	0.2049	-0.0001	0.2648	0.2648
13	81.00	-349.980	-0.095	-350.008	-350.125	0.2648	-0.0000	0.2648	0.2648
14	85.00	-350.755	-0.772	-351.295	-351.145	0.2647	-0.0001	0.2315	0.1699
15	89.00	-350.734	0.299	-350.409	-350.207	0.1368	0.0000	0.1368	0.1368
16	93.00	-350.092	0.062	-350.030	-350.000	0.1368	0.0000	0.1369	0.1369
17	97.00	-349.986	0.006	-349.981	-349.979	0.1369	0.0000	0.1369	0.1369
18	102.00	-349.979	0.000	-349.979	-349.979	0.1369	0.0000	0.1369	0.1369
19	107.00	-349.980	-0.001	-349.979	-349.978	0.1369	-0.0000	0.1369	0.1369
20	112.00	-349.979	-0.001	-349.980	-349.980	0.1369	-0.0000	0.1369	0.1369
21	116.00	-349.982	-0.002	-349.982	-349.980	0.1369	-0.0000	0.1369	0.1369
22	125.00	-349.982	-0.002	-349.982	-349.980	0.1369	-0.0000	0.1369	0.1369
23	133.00	-349.982	-0.002	-349.982	-349.980	0.1369	-0.0000	0.1369	0.1369
24	141.00	-349.981	-0.001	-349.982	-349.980	0.1369	-0.0000	0.1369	0.1369
25	150.00	-349.980	-0.001	-349.982	-349.983	0.1369	-0.0000	0.1369	0.1369
26	160.00	-349.984	-0.000	-349.985	-349.988	0.1369	-0.0000	0.1369	0.1369
27	170.00	-349.990	0.0			0.1369	0.0		

INFILTRATION RATE(CM/DAY)..... 25.000
DRAINAGE RATE(CM/DAY)..... 0.008
TOTAL MOISTURE IN PROFILE(CM3)... 34.966

MOISTURE ADDED TO PROFILE (CM3)..... 2.427
MOISTURE INCREASE IN PROFILE(CM3).... 2.412
DEVIATION(CM3)..... 0.015

****

ELAPSED TIME	DAYS	HOURS	MINUTES	SECONDS	TIME STEP	STEP #	NIT	NITT
	0.1540	3.695	0.2217E 03	0.1330E 05	0.11369E-01	32	3	78

		PRESSURE HEAD				MOISTURE CONTENT			
NODE	DEPTH	FUNCTION	GRADIENT	F(-1/3)	F(+1/3)	FUNCTN	GRADNT	F(-1/3)	F(+1/3)
1	0.0	-41.289	-1.749	-44.916	-46.969	0.5212	-0.0015	0.5185	0.5153
2	6.00	-53.696	-2.574	-60.979	-69.694	0.5114	-0.0021	0.5052	0.4976
3	14.00	-83.742	-4.693	-94.438	-112.859	0.4878	-0.0042	0.4756	0.4596
4	22.00	-139.546	-12.000	-164.965	-195.031	0.4386	-0.0090	0.3959	0.3315
5	28.00	-232.454	-21.003	-267.148	-329.909	0.2886	-0.0090	0.2592	0.2384
6	36.00	-346.779	0.274	-347.252	-348.789	0.2255	0.0001	0.2156	0.2055
7	46.00	-348.329	0.469	-348.177	-348.376	0.1957	0.0001	0.1884	0.1809
8	55.00	-348.435	0.115	-348.327	-348.446	0.1734	0.0000	0.1676	0.1618
9	63.00	-348.542	0.000	-348.578	-348.635	0.1559	0.0000	0.1520	0.1481
10	69.00	-348.634	0.029	-348.578	-348.465	0.1442	0.0000	0.1416	0.1394
11	73.00	-348.264	0.192	-347.962	-347.921	0.1370	0.0000	0.1702	0.2318
12	77.00	-348.670	-0.990	-349.561	-349.863	0.2049	-0.0001	0.2648	0.2648
13	81.00	-349.974	-0.112	-350.078	-350.339	0.2648	-0.0000	0.2648	0.2648
14	85.00	-351.135	-0.890	-351.757	-351.585	0.2647	-0.0001	0.2315	0.1699
15	89.00	-351.114	0.341	-350.721	-350.440	0.1368	0.0000	0.1368	0.1368
16	93.00	-350.253	0.111	-350.132	-350.060	0.1368	0.0000	0.1368	0.1368
17	97.00	-350.020	0.022	-349.993	-349.982	0.1369	0.0000	0.1369	0.1369
18	102.00	-349.979	0.001	-349.977	-349.977	0.1369	0.0000	0.1369	0.1369
19	107.00	-349.977	-0.000	-349.976	-349.975	0.1369	-0.0000	0.1369	0.1369

20	112.00	-349.976	-0.001	-349.976	-349.975	0.1369	-0.0000	0.1369	0.1369
21	118.00	-349.976	-0.001	-349.977	-349.976	0.1369	-0.0000	0.1369	0.1369
22	125.00	-349.977	-0.001	-349.977	-349.976	0.1369	-0.0000	0.1369	0.1369
23	133.00	-349.976	-0.001	-349.976	-349.975	0.1369	-0.0000	0.1369	0.1369
24	141.00	-349.976	-0.001	-349.976	-349.974	0.1369	-0.0000	0.1369	0.1369
25	150.00	-349.976	-0.002	-349.978	-349.977	0.1369	-0.0000	0.1369	0.1369
26	160.00	-349.978	-0.001	-349.982	-349.986	0.1369	-0.0000	0.1369	0.1369
27	170.00	-349.989	0.0			0.1369	0.0		

INFILTRATION RATE(CM/DAY)..... 25.000
DRAINAGE RATE(CM/DAY)..... 0.008
TOTAL MOISTURE IN PROFILE(CM3)... 36.388

MOISTURE ADDED TO PROFILE (CM3)..... 3.848
MOISTURE INCREASE IN PROFILE(CM3).... 3.834
DEVIATION(CM3)..... 0.013

****

ELAPSED TIME	DAYS	HOURS	MINUTES	SECONDS	TIME STEP	STEP #	NIT	NITT
	0.2023	4.855	0.2913E 03	0.1748E 05	0.1421IE-01	36	3	89

		PRESSURE HEAD				MOISTURE CONTENT			
NODE	DEPTH	FUNCTION	GRADIENT	F(-1/3)	F(+1/3)	FUNCTN	GRADNT	F(-1/3)	F(+1/3)
1	0.0	-33.766	-1.311	-36.439	-39.363	0.5266	-0.0009	0.5248	0.5227
2	6.00	-42.758	-1.852	-47.934	-53.954	0.5201	-0.0014	0.5161	0.5112
3	14.00	-61.375	-3.115	-70.275	-81.683	0.5049	-0.0027	0.4971	0.4869
4	22.00	-97.583	-7.053	-111.130	-124.100	0.4729	-0.0062	0.4378	0.3822
5	28.00	-137.302	-6.794	-157.651	-183.866	0.3466	-0.0057	0.3220	0.2950
6	36.00	-218.047	-14.574	-275.595	-329.734	0.2066	-0.0071	0.2334	0.2093
7	46.00	-348.445	2.903	-345.302	-347.985	0.1958	0.0005	0.1889	0.1809
8	55.00	-348.530	1.059	-347.361	-348.002	0.1734	0.0002	0.1677	0.1618
9	63.00	-348.197	0.292	-347.988	-348.167	0.1560	0.0000	0.1521	0.1482
10	69.00	-348.189	0.119	-348.070	-347.964	0.1443	0.0000	0.1419	0.1395
11	73.00	-347.767	0.207	-347.452	-347.437	0.1371	0.0000	0.1703	0.2319
12	77.00	-348.282	-1.096	-349.319	-349.757	0.2649	-0.0001	0.2649	0.2648
13	81.00	-349.965	-0.163	-350.157	-350.527	0.2648	-0.0000	0.2648	0.2648
14	85.00	-351.421	-0.952	-352.067	-351.904	0.2647	-0.0001	0.2315	0.1699
15	89.00	-351.402	0.363	-350.972	-350.645	0.1367	0.0000	0.1368	0.1368
16	93.00	-350.409	0.145	-350.247	-350.137	0.1368	0.0000	0.1368	0.1368
17	97.00	-350.069	0.039	-350.019	-349.994	0.1368	0.0000	0.1369	0.1369
18	102.00	-349.983	0.005	-349.977	-349.975	0.1369	0.0000	0.1369	0.1369
19	107.00	-349.975	0.000	-349.973	-349.973	0.1369	0.0000	0.1369	0.1369
20	112.00	-349.973	-0.000	-349.973	-349.971	0.1369	-0.0000	0.1369	0.1369
21	118.00	-349.972	-0.001	-349.973	-349.972	0.1369	-0.0000	0.1369	0.1369
22	125.00	-349.973	-0.001	-349.973	-349.972	0.1369	-0.0000	0.1369	0.1369
23	133.00	-349.972	-0.001	-349.972	-349.970	0.1369	-0.0000	0.1369	0.1369
24	141.00	-349.971	-0.001	-349.971	-349.971	0.1369	-0.0000	0.1369	0.1369
25	150.00	-349.973	-0.002	-349.975	-349.973	0.1369	-0.0000	0.1369	0.1369
26	160.00	-349.974	-0.001	-349.979	-349.985	0.1369	-0.0000	0.1369	0.1369
27	170.00	-349.987	0.0			0.1369	0.0		

INFILTRATION RATE(CM/DAY)..... 25.000
DRAINAGE RATE(CM/DAY)..... 0.008
TOTAL MOISTURE IN PROFILE(CM3)... 37.599

MOISTURE ADDED TO PROFILE (CM3)..... 5.056
MOISTURE INCREASE IN PROFILE(CM3).... 5.045
DEVIATION(CM3)..... 0.011

Table A5. Listing of UNSAT1.

```
C
C
C        ***************************************************************
C        *                                                             *
C        *          ONE-DIMENSIONAL UNSATURATED FLOW                   *
C        *          HERMITIAN BASIS FUNCTIONS                  SLP     *
C        *                                                             *
C        *          UNSAT1                                             *
C        *                                          NOVEMBER 1978      *
C        *                                                             *
C        ***************************************************************
C
C
C
      COMMON /ONE/ X(30), ISPR(30), INT(30), P(60), PE(60)
      DIMENSION T(60)
      DATA NITMAX/10/
C
C     ----- OBTAIN INITIAL CONDITIONS AND PROGRAM CONSTANTS -----
      CALL DATAIN(NN,KOD1,KRAIN,KDRAIN,NSTEPS,TMAX,DELT,DELMAX,DELMIN,
     1PRDEL,PULSE,EPSI,TMINIT,DRAIN,TOL1,TOL2)
C
C     ----------
      NN2=2*NN
      N1=NN2-1
      NITT=0.
      TMINF=0.
      PRTIME=0.
      SUMT=DELT
      ISTEP=1
      DO 8 I=1,NN2
    8 PE(I)=P(I)
C
C     ----- DYNAMIC PART OF MODEL -----
    9 NIT=0
   10 NIT=NIT+1
      NITT=NITT+1
      IF(SUMT.GE.PULSE) KRAIN=1
      DO 12 I=1,NN2
   12 T(I)=PE(I)
      CALL MATEQ(NN,KRAIN,KDRAIN,DELT,SUMT,EPSI,RAIN,DRAIN)
      IF(KOD1.EQ.1) WRITE(6,1002) NIT,DELT,ISTEP,SUMT,(PE(I),I=1,NN2)
C
C     ----- CHECK ITERATIVE PROCESS -----
      DO 14 I=1,NN2,2
      TOL=TOL1+TOL2*ABS(T(I))
      IF(ABS(PE(I)-T(I))-TOL) 14,14,16
   14 CONTINUE
      GO TO 26
   16 IF(NIT-NITMAX) 10,18,18
   18 DELT=0.5*DELT
      WRITE(6,1006) NIT,SUMT,DELT
```

```
      IF(DELT.GE.DELMIN) GO TO 22
      WRITE(6,1008) DELT,DELMIN,SUMT
      DO 20 I=1,NN
      J=2*I-1
   20 WRITE(6,1010) I,X(I),P(J),P(J+1),PE(J),PE(J+1)
      CALL EXIT
   22 SUMT=SUMT-DELT
      DO 24 I=1,NN2
   24 PE(I)=0.5*(P(I)+PE(I))
      GO TO 9
C
C     ----------
   26 PRTIME=PRTIME+DELT
      IF(KRAIN) 28,28,30
   28 MAT=ISPR(1)
      EL=X(2)-X(1)
      P1=.957031*P(1)+.042969*P(3)+EL*(.095703*P(2)-.013672*P(4))
      PE1=.957031*PE(1)+.042969*PE(3)+EL*(.095703*PE(2)-.013672*PE(4))
      P2=.65625*(P(3)-P(1))/EL+.546875*P(2)-.203125*P(4)
      PE2=.65625*(PE(3)-PE(1))/EL+.546875*PE(2)-.203125*PE(4)
      RAIN=0.5*(SPR(MAT,2,P1)*(1.-P2)+SPR(MAT,2,PE1)*(1.-PE2))
   30 IF(KDRAIN.EQ.2) GO TO 32
      MAT=ISPR(NN)
      DRAIN=0.5*(SPR(MAT,2,P(N1))*(1.-P(NN2))+SPR(MAT,2,PE(N1))*(1.-PE(N
     1N2)))
   32 TMINF=TMINF+(RAIN-DRAIN)*DELT
C
C     ----- CHECK FOR POSSIBLE PRINT-OUT -----
      IF(PRTIME.LT.(PRDEL-0.5*DELT)) GO TO 34
      PRTIME=PRTIME-PRDEL
      IF(KRAIN.EQ.0) RAIN=SPR(ISPR(1),2,PE1)*(1.-PE2)
      IF(KRAIN.EQ.1) RAIN=BC(2,SUMT)
      IF(KDRAIN.NE.2) DRAIN=SPR(ISPR(NN),2,PE(N1))*(1.-PE(NN2))
      CALL PRINT(NN,RAIN,DRAIN,SUMT,ISTEP,NIT,NITT,DELT,TMINIT,TMINF)
C
C     ----- PREPARE FOR THE NEXT TIME STEP -----
   34 IF(SUMT.GE.TMAX.OR.ISTEP.GE.NSTEPS) GO TO 38
      DELCH=1.0
      IF(NIT.LE.2) DELCH=1.25
      IF(NIT.GE.6) DELCH=0.80
      DELCH=AMIN1(DELCH,DELMAX/DELT)
      DELT=DELT*DELCH
      SUMT=SUMT+DELT
      ISTEP=ISTEP+1
      DO 36 J=1,NN2
      PE1=DELCH*(PE(J)-P(J))
      P(J)=PE(J)
   36 PE(J)=P(J)+PE1
      GO TO 9
   38 WRITE (6,1012) SUMT,ISTEP
      STOP
```

```
C
C     ---------------
 1002 FORMAT(/11X,'PE(I) DURING ITERATION (NIT=',I3,' DELT =',F10.6,' IS
     1TEP =',I4,' SUMT =',F10.5,')'/(10X,10F11.3))
 1006 FORMAT(//11X,10(1H*),'NO CONVERGENCE AFTER',I3,' ITERATIONS AT TIM
     1E =',F8.5,' NEW DELT =',E11.4,1X,10(1H*))
 1008 FORMAT(//11X,8(1H*),'DELT =',E11.4,', IS LESS THAN DELMIN (=',E11.
     14,'), EXECUTION TERMINATED AT TIME =',E11.4,1X,10(1H*)//11X,'LAST
     2CALCULATED VALUES'/11X,22(1H*)/11X,'NODE',5X,'DEPTH',9X,'P(I)',6X,
     3'GRADIENT',9X,'PE(I)',6X,'GRADIENT')
 1010 FORMAT(11X,I4,F10.2,2(3X,2F12.4))
 1012 FORMAT(//11X,10(14*),'NORMAL TERMINATION AT TIME =',F13.5,' DAYS A
     1ND STEP NUMBER =',I5)
      END
```

```
      SUBROUTINE BANSOL(NEQ)
C
C     PURPOSE: TO SOLVE THE GLOBAL MATRIX EQUATION
C
      COMMON /TWO/ S(60,4), F(60)
      N1=NEQ-1
      DO 4 I=1,N1
      J=I-1
      M=MIN0(4,NEQ-J)
      P=S(I,1)
      DO 4 L=2,M
      C=S(I,L)/P
      II=J+L
      JJ=0
      DO 2 K=L,M
      JJ=JJ+1
    2 S(II,JJ)=S(II,JJ)-C*S(I,K)
    4 S(I,L)=C
      DO 6 I=1,N1
      J=I-1
      M=MIN0(4,NEQ-J)
      C=F(I)
      F(I)=C/S(I,1)
      DO 6 L=2,M
      II=J+L
    6 F(II)=F(II)-S(I,L)*C
      F(NEQ)=F(NEQ)/S(NEQ,1)
      DO 8 I=1,N1
      II=NEQ-I
      J=II-1
      M=MIN0(4,NEQ-J)
      DO 8 K=2,M
      L=J+K
    8 F(II)=F(II)-S(II,K)*F(L)
      RETURN
      END
```

BC

```
      FUNCTION BC(K,SUMT)
C
C     PURPOSE: TO CALCULATE TRANSIENT BOUNDARY CONDITIONS
C
      DIMENSION TO(2),RO(2),T1(4),R1(4)
      DATA N1/2/, TO/0.,100./, RO/-14.4954,-14.4954/
      DATA N2/4/, T1/0.,0.49,0.51,100./, R1/25.,25.,-0.5,-0.5/
C
C     ----------
      IF(K.EQ.2) GO TO 6
      DO 2 I=2,N1
      IF(TO(I)-SUMT) 2,4,4
    2 CONTINUE
    4 BC=((TO(I)-SUMT)*RO(I-1)+(SUMT-TO(I-1))*RO(I))/(TO(I)-TO(I-1))
      RETURN
    6 DO 8 I=2,N2
      IF(T1(I)-SUMT) 8,10,10
    8 CONTINUE
   10 BC=((T1(I)-SUMT)*R1(I-1)+(SUMT-T1(I-1))*R1(I))/(T1(I)-T1(I-1))
      RETURN
      END
```

DATAIN

```
      SUBROUTINE DATAIN(NN,KOD1,KRAIN,KORAIN,NSTEPS,TMAX,DELT,DELMAX,
     1DELMIN,PROEL,PULSE,EPSI,TMINIT,DRAIN,TOL1,TOL2)
C
C     PURPOSE: DEFINE GEOMETRY AND INITIAL CONDITIONS
C
      COMMON /ONE/ X(30), ISPR(30), INT(30), P(60), PE(60)
      DIMENSION TITLE(20), A(5), B(5)
C
C     ---------------
      WRITE(6,1000)
      DO 1 I=1,3
      READ(5,1002) TITLE
    1 WRITE(6,1004) TITLE
      WRITE(6,1006)
      READ(5,1008) NN,NSTEPS,DELT,DELMIN,DELMAX,TMAX,PROEL,PULSE,EPSI
      READ(5,1010) KRAIN,KORAIN,KOD1,KOD2,KOD3,DRAIN,TOL1,TOL2
      WRITE(6,1012) NN,NSTEPS,DELT,DELMIN,DELMAX,TMAX,PROEL,PULSE,EPSI
C
C     ----- READ INITIAL CONDITIONS -----
      DO 6 I=1,NN
      READ(5,1016) K,MAT,X(K),Z1,Z2,INT(K)
      IF(K.EQ.I) GO TO 2
      WRITE(6,1018) I
      CALL EXIT
    2 J=2*I-1
      J1=J+1
      ISPR(I)=MAT
      IF(KOD2.EQ.0) GO TO 4
      P(J)=Z1
      P(J1)=Z2
      GO TO 6
    4 P(J)=SPR(MAT,4,Z1)
      P(J1)=Z2/SPR(MAT,3,P(J))
    6 CONTINUE
C
C     ----- REDEFINE SURFACE PRESSURE VALUES IF KRAIN=1 -----
      NN2=2*NN
      EL=X(2)-X(1)
      IF(KRAIN.EQ.0) GO TO 12
      RAIN=BC(2,0.)
      MAT=ISPR(1)
      WRITE(6,1020)
      Z1=SPR(MAT,1,P(1))
      Z2=Z1
      Z3=SPR(MAT,3,P(1))*P(2)
      Z4=AMIN1(0.5,100./EL)
      P(2)=1.-RAIN/SPR(MAT,2,P(1))
      I=0
    8 I=I+1
      IF(I.LT.40) GO TO 10
      WRITE(6,1022)
```

```
      CALL EXIT
   10 WC=Z1-EL*(SPR(MAT,3,P(1))*P(2)-Z3)/6.
      Z2=(1.-Z4)*Z2+Z4*WC
      P(1)=SPR(MAT,4,Z2)
      P(2)=1.-RAIN/SPR(MAT,2,P(1))
      WRITE(6,1024) I,Z2,P(1),P(2)
      IF(ABS(Z2-WC)-0.0001) 14,14,8
   12 P(1)=BC(1,0.)
      P(2)=3*(P(3)-P(1))/EL
      RAIN=SPR(ISPR(1),2,P(1))*(1.-P(2))
   14 CONTINUE
      IF(KORAIN-2) 15,16,15
   15 DRAIN=SPR(ISPR(NN),2,P(NN2-1))*(1.-P(NN2))
      GO TO 17
   16 P(NN2)=1.-DRAIN/SPR(ISPR(NN),2,P(NN2-1))
   17 WRITE(6,1014) TOL1,TOL2,RAIN,DRAIN,KRAIN,KORAIN,KOD1,KOD2,KOD3
C
C     ----- WRITE INITIAL CONDITIONS -----
      TMINIT=0.
      WRITE(6,1026)
      NE=NN-1
      DO 18 L=1,NE
      G1=.7407407-.0740741*FLOAT(INT(L))
      G2=1.-G1
      MAT=ISPR(L)
      MAT1=ISPR(L+1)
      I=2*L-1
      I1=I+1
      I2=I+2
      I3=I+3
      EL=X(L+1)-X(L)
      P13=.7407407*P(I)+.2592593*P(I2)+.0740741*EL*(2.*P(I1)-P(I3))
      P23=.2592593*P(I)+.7407407*P(I2)+.0740741*EL*(P(I1)-2.*P(I3))
      Z1=SPR(MAT,1,P(I))
      Z2=SPR(MAT,3,P(I))*P(I1)
      Z3=G1*SPR(MAT,1,P13)+G2*SPR(MAT1,1,P13)
      Z4=G2*SPR(MAT,1,P23)+G1*SPR(MAT1,1,P23)
      Z5=SPR(MAT1,1,P(I2))
      WRITE(6,1028) L,X(L),P(I),P(I1),P13,P23,Z1,Z2,Z3,Z4,MAT,INT(L)
   18 TMINIT=TMINIT+EL*(0.5*(Z1+Z5)+Z3+Z4)/3.
      Z2=SPR(MAT1,3,P(I2))*P(NN2)
      WRITE(6,1030) NN,X(NN),P(I2),P(NN2),Z5,Z2,MAT1
      WRITE(6,1032) TMINIT
C
C     ----- CALCULATE MATERIAL PROPERTIES -----
      IF(KOD3.EQ.0) GO TO 24
      I1=(KOD3-1)/5+1
      DO 22 I=1,I1
      I2=5*I
      I3=I2-4
      WRITE(6,1034) (K,K=I3,I2)
```

```
      I2=MINO(I2,KOD3-I2+5)
      Z1=-0.5
      DO 20 J=1,54
      Z1=Z1*1.2
      DO 19 J1=1,I2
      K=J1+5*(I-1)
      A(J1)=SPR(K,1,Z1)
   19 B(J1)=SPR(K,2,Z1)
   20 WRITE(6,1036) Z1,(A(K),B(K),K=1,I2)
   22 CONTINUE
      WRITE(6,1038)
   24 CONTINUE
C
C     ---------------
 1000 FORMAT(1H1,10X, 82(1H*)/11X,1H*,80X,1H*/11X,1H*,9X,'ONE-DIMENSIONA
     1L SATURATED-UNSATURATED FLOW',29X,1H*/11X,1H*,80X,1H*)
 1002 FORMAT(20A4)
 1004 FORMAT(11X,1H*,20A4,1H*)
 1006 FORMAT(11X,1H*,80X,1H*/11X,82(1H*))
 1008 FORMAT(2I5,7F10.0)
 1010 FORMAT(5I5,4F10.0)
 1012 FORMAT(//11X,'INPUT PARAMETERS'/11X,16(1H=)/11X,
     1'NUMBER OF NODES.....(NN).....',I5/11X,
     2'MAXIMUM NUMBER OF TIME STEPS.....(NSTEPS).....',I5/11X,
     3'INITIAL TIME STEP.....(DELT).....',E11.5/11X,
     4'MINIMUM ALLOWABLE TIME STEP.....(DELMIN).....',E11.5/11X,
     5'MAXIMUM ALLOWABLE TIME STEP.....(DELMAX).....',E11.5/11X,
     6'MAXIMUM SIMULATION TIME.....(TMAX).....',F10.3/11X,
     7'PRINT DELT FOR OUTPUT.....(PRDEL).....',F10.3/11X,
     8'PULSE LENGTH FOR 1ST-TYPE BC.....(PULSE).....',F10.3/11X,
     9'WEIGHTING COEFFICIENT.....(EPSI).....',F10.3)
 1014 FORMAT(//11X,'ADDITIONAL PARAMETERS'/11X,21(1H=)/11X,
     1'ITERATION TOLERANCE.....(TOL1).....',F10.3/11X,
     2'ITERATION TOLERANCE.....(TOL2).....',F10.3/11X,
     3'INITIAL INFILTRATION RATE.....(RAIN).....',F10.3/11X,
     4'INITIAL DRAINAGE RATE.....(DRAIN).....',F10.3/11X,
     5'KRAIN.....(RAINFALL CODE).....',I5/11X,
     6'KORAIN.....(DRAINAGE CODE).....',I5/11X,
     7'KOD1.....(OUTPUT FOR EVERY ITERATION).....',I5/11X,
     8'KOD2.....(INPUT VARIABLE IS PRESSURE HEAD).....',I5/11X,
     9'KOD3.....(WRITE MATERIAL PROPERTIES).....',I5/1H1)
 1016 FORMAT(2I5,3F10.0,I5)
 1018 FORMAT(//5X,8(1H*),'ERROR ENCOUNTERED WHILE READING INITIAL CONDIT
     1IONS, CHECK NODE',I4,1X,'EXECUTION TERMINATED',9(1H*))
 1020 FORMAT(//11X,'REDEFINED SURFACE VALUES'/11X,24(1H=)/11X,'ITERATION
     1',7X,'MOIST. CONT.',4X,'PRESSURE',4X,'GRADIENT')
 1022 FORMAT(//8X,9(1H*),'PROBLEMS ENCOUNTERED WHILE REDEFINING SURFACE
     1PRESSURE VALUES, EXECUTION TERMINATED',1X,9(1H*))
 1024 FORMAT(13X,I4,8X,F11.4,5X,F10.3,3X,F10.4)
 1026 FORMAT(//11X,'INITIAL CONDITIONS'/11X,18(1H=)/27X,14(1H-),'PRESSUR
     1E HEAD',12(1H-),6X, 8(1H-),'MOISTURE CONTENT', 9(1H-),5X,'INDICES'
```

```
     2 /11X,'NODE',2X,'DEPTH',3X,'FUNCTION',3X,'GRADIENT',4X,'F(-1/3)',4
     3X,'F(+1/3)',6X,'FUNCTN',3X,'GRADNT',2X,'F(-1/3)',2X,'F(+1/3)',4X,'
     4MAT',2X,'INT')
1028 FORMAT(10X,I4,1X,F7.2,4F11.3,3X,4F9.4,1X,2I5)
1030 FORMAT(10X,I4,1X,F7.2,2F11.3,25X,2F9.4,19X,I5)
1032 FORMAT(//11X,'INITIAL AMOUNT OF MOISTURE IN PROFILE:',F9.4,' CM3')
1034 FORMAT(1H1,10X,'SOIL-HYDRAULIC PROPERTIES (MOISTURE CONTENT AND HY
     1DRAULIC CONDUCTIVITY)'/11X,71(1H=)//13X,5(16X,'SOIL')/11X,'PRESSUR
     2E',10X,I3,4(17X,I3)/13X,'HEAD',5(8X,'MC',6X,'COND'))
1036 FORMAT(10X,E10.3,1X,5(2X,F7.4,E11.3))
1038 FORMAT(1H1)
      RETURN
      END
```

MATEQ

```
      SUBROUTINE MATEQ(NN,KRAIN,KDRAIN,DELT,SUMT,EPSI,RAIN,DRAIN)
C
C     PURPOSE: TO CALCULATE THE GLOBAL MATRIX EQUATION
C
      COMMON /ONE/ X(30), ISPR(30), INT(30), P(60), PE(60)
      COMMON /TWO/ S(60,4), F(60)
      DIMENSION FE(4,3), DX(4,3), SR(10), T(60)
      DATA FE(1,1),FE(3,3),FE(1,2),FE(3,2),FE(1,3),FE(3,1),DX(1,1),DX(1,
     13),DX(1,2),DX(3,2),DX(3,1),DX(3,3)/2*.9209488,2*0.5,2*.0791512,2*-
     2.4285714,-.75,.75,2*.4285714/
C
C     ----------
      NE=NN-1
      NN2=2*NN
      N1=NN2-1
      N2=NN2-2
      N3=NN2-3
      NEQ=N1-KDRAIN/3
      EPSM=EPSI-1.
      DO 2 I=1,NN2
      T(I)=0.5*(P(I)+PE(I))
      DO 2 J=2,4
    2 S(I,J)=0.
C
C     ----- CONTRIBUTIONS OF NODAL INTEGRATION POINTS -----
      DO 4 I=1,NN
      LL=2*I-1
      L1=LL+1
      II=MAXO(I-1,1)
      JJ=MINO(I+1,NN)
      EL1=0.05*(X(JJ)-X(II))
      MAT=ISPR(I)
      CAP1=SPR(MAT,3,T(LL))*EL1/DELT
      COND1=SPR(MAT,2,T(LL))*EL1
      S(LL,1)=CAP1
      S(L1,1)=EPSI*COND1
      F(LL)=CAP1*P(LL)
    4 F(L1)=(EPSM*P(L1)+1.)*COND1
C
C     ----- ELEMENT LOOP; CONSTRUCT GLOBAL MATRIX -----
      DO 12 L=1,NE
      LL=2*L-2
      L1=LL+1
      L2=LL+2
      L3=LL+3
      L4=LL+4
      EL=X(L+1)-X(L)
C
C     ----- CALCULATE HERMITIAN BASIS FUNCTIONS -----
      FE(2,1)=.1181895*EL
      FE(2,2)=.125*EL
```

```
      FE(2,3)=.0246676*EL
      DX(2,1)=.1993777*EL
      DX(2,2)=-.125*EL
      DX(2,3)=-.1279491*EL
      DO 6 K=1,3
      FE(4,K)=-FE(2,4-K)
    6 DX(4,K)=DX(2,4-K)
C
C     ----- CALCULATE MATERIAL PROPERTIES AT LOBATTO POINTS -----
      W1=FE(1,1)*T(L1)+FE(2,1)*T(L2)+FE(3,1)*T(L3)+FE(4,1)*T(L4)
      W2=FE(1,2)*T(L1)+FE(2,2)*T(L2)+FE(3,2)*T(L3)+FE(4,2)*T(L4)
      W3=FE(1,3)*T(L1)+FE(2,3)*T(L2)+FE(3,3)*T(L3)+FE(4,3)*T(L4)
      MAT1=ISPR(L)
      MAT2=ISPR(L+1)
      G2=.0861869+.101835*FLOAT(INT(L))
      G1=1.088889-G2
      COND1=(G1*SPR(MAT1,2,W1)+G2*SPR(MAT2,2,W1))/EL
      COND2=.7111111*(SPR(MAT1,2,W2)+SPR(MAT2,2,W2))/EL
      COND3=(G2*SPR(MAT1,2,W3)+G1*SPR(MAT2,2,W3))/EL
      EL1=.25*EL/DELT
      CAP1=(G1*SPR(MAT1,3,W1)+G2*SPR(MAT2,3,W1))*EL1
      CAP2=.7111111*(SPR(MAT1,3,W2)+SPR(MAT2,3,W2))*EL1
      CAP3=(G2*SPR(MAT1,3,W3)+G1*SPR(MAT2,3,W3))*EL1
C
C     ----- ADD ELEMENT CONTRIBUTIONS TO GLOBAL MATRIX -----
      K=0
      DO 10 I=1,4
      II=LL+I
      DO 10 J=I,4
      W1=DX(J,1)*DX(I,1)*COND1+DX(J,2)*DX(I,2)*COND2+DX(J,3)*DX(I,3)*
     1COND3
      W2=FE(J,1)*FE(I,1)*CAP1+FE(J,2)*FE(I,2)*CAP2+FE(J,3)*FE(I,3)*CAP3
      JJ=J+1-I
      K=K+1
      S(II,JJ)=S(II,JJ)+W1*EPSI+W2
   10 SR(K)=W1*EPSM+W2
C
C     ----- CONSTRUCT RHS VECTOR ----
      EL1=.2142857*EL*(COND1+1.75*COND2+COND3)
      F(L1)=F(L1)+SR(1)*P(L1)+SR(2)*P(L2)+SR(3)*P(L3)+SR(4)*P(L4)-EL1
      F(L2)=F(L2)+SR(2)*P(L1)+SR(5)*P(L2)+SR(6)*P(L3)+SR(7)*P(L4)+
     1(.0996889*COND1-.0625*COND2-.0639746*COND3)*EL*EL
      F(L3)=F(L3)+SR(3)*P(L1)+SR(6)*P(L2)+SR(8)*P(L3)+SR(9)*P(L4)+EL1
   12 F(L4)=F(L4)+SR(4)*P(L1)+SR(7)*P(L2)+SR(9)*P(L3)+SR(10)*P(L4)+
     1(.0996889*COND3-.0625*COND2-.0639746*COND1)*EL*EL
C
C     ----- INCLUDE BOUNDARY CONDITIONS -----
      IF(KRAIN.EQ.1) GO TO 22
      S(1,1)=1.
      F(1)=BC(1,SUMT)
      DO 20 I=2,4
```

```
      F(I)=F(I)-S(1,I)*F(1)
   20 S(1,I)=0.
      GO TO 24
   22 S(2,1)=1.
      W1=AMIN1(0.5,100./(X(2)-X(1)))
      W2=1.-BC(2,SUMT)/SPR(ISPR(1),2,PE(1))
      F(2)=(1.-W1)*PE(2)+W1*W2
      RAIN=(BC(2,SUMT)+BC(2,SUMT-0.5*DELT)+BC(2,SUMT-DELT))/3.
      F(1)=F(1)-S(1,2)*F(2)+RAIN
      F(3)=F(3)-S(2,2)*F(2)
      F(4)=F(4)-S(2,3)*F(2)
      S(1,2)=0.
      S(2,2)=0.
      S(2,3)=0.
   24 CONTINUE
      IF(KDRAIN-2) 26,28,30
   26 IF(KDRAIN.EQ.0) GO TO 27
      MAT=ISPR(NN)
      DRAIN=0.5*(SPR(MAT,2,P(N1))+SPR(MAT,2,PE(N1)))*(1.-P(NN2))
      GO TO 29
   27 F(N1)=F(NN2)-S(N1,2)*P(N1)
      F(N2)=F(N2)-S(N2,2)*P(N1)
      F(N3)=F(N3)-S(N3,3)*P(N1)
      S(N1,1)=S(NN2,1)
      S(N2,2)=S(N2,3)
      S(N3,3)=S(N3,4)
      GO TO 32
   28 PE(NN2)=0.5*(PE(NN2)+1.-DRAIN/SPR(ISPR(NN),2,PE(N1)))
   29 F(N1)=F(N1)-S(N1,2)*PE(NN2)-DRAIN
      F(N2)=F(N2)-S(N2,3)*PE(NN2)
      F(N3)=F(N3)-S(N3,4)*PE(NN2)
      GO TO 32
   30 F(N2)=F(N2)-S(N2,2)*P(N1)-S(N2,3)*P(NN2)
      F(N3)=F(N3)-S(N3,3)*P(N1)-S(N3,4)*P(NN2)
   32 CONTINUE
C
C     ----- SOLVE FOR UNKNOWNS -----
      CALL BANSOL(NEQ)
C
C     ----------
      DO 34 I=1,N2
   34 PE(I)=F(I)
      IF(KDRAIN.EQ.0) PE(NN2)=F(N1)
      IF(KDRAIN.EQ.1) PE(N1)=F(N1)
      RETURN
      END
```

```
      SUBROUTINE PRINT(NN,RAIN,DRAIN,SUMT,ISTEP,NIT,NITT,DELT,TMINIT,
     1TMINF)
C
C     PURPOSE: PRINT PRESSURE HEAD AND MOISTURE CONTENT VS DEPTH
C
      COMMON /ONE/ X(30), ISPR(30), INT(30), P(60), PE(60)
C
C     ----------
      NE=NN-1
      SUMT1=SUMT*24.
      SUMT2=SUMT1*60.
      SUMT3=SUMT2*60.
      WRITE(6,1002) SUMT,SUMT1,SUMT2,SUMT3,DELT,ISTEP,NIT,NITT
      TMIN=0.
      DO 4 L=1,NE
      EL=X(L+1)-X(L)
      G1=.7407407-.0740741*FLOAT(INT(L))
      G2=1.-G1
      I=2*L-1
      I1=I+1
      I2=I+2
      I3=I+3
      MAT1=ISPR(L)
      MAT2=ISPR(L+1)
      P13=.7407407*PE(I)+.2592593*PE(I2)+.0740741*EL*(2.*PE(I1)-PE(I3))
      P23=.2592593*PE(I)+.7407407*PE(I2)+.0740741*EL*(PE(I1)-2.*PE(I3))
      Z1=SPR(MAT1,1,PE(I))
      Z2=SPR(MAT1,3,PE(I))*PE(I1)
      Z3=G1*SPR(MAT1,1,P13)+G2*SPR(MAT2,1,P13)
      Z4=G2*SPR(MAT1,1,P23)+G1*SPR(MAT2,1,P23)
      Z5=SPR(MAT2,1,PE(I2))
      WRITE(6,1004) L,X(L),PE(I),PE(I1),P13,P23,Z1,Z2,Z3,Z4
    4 TMIN=TMIN+EL*(0.5*(Z1+Z5)+Z3+Z4)/3.
      Z2=SPR(MAT2,3,PE(I2))*PE(I3)
      WRITE(6,1006) NN,X(NN),PE(I2),PE(I3),Z5,Z2
      TMINCR=TMIN-TMINIT
      TMDIFF=TMINF-TMINCR
      WRITE(6,1008) RAIN,TMINF,DRAIN,TMINCR,TMIN,TMDIFF
C
C     ----------
 1002 FORMAT(//11X,103(1H*)/11X,'ELAPSED TIME',5X,'DAYS',7X,'HOURS',6X,
     1'MINUTES',5X,'SECONDS',6X,'TIME STEP',5X,'STEP #',4X,'NIT',3X,'NIT
     2T'/21X,F13.4,F10.3,E14.4,E14.4,4X,E12.5,4X,I4,4X,I4,3X,I5//29X,14(
     31H-),'PRESSURE HEAD',14(1H-),8X,10(1H-),'MOISTURE CONTENT',10(1H-)
     4/11X,'NODE',5X,'DEPTH',4X,'FUNCTION',3X,'GRADIENT',4X,'F(-1/3)',4X
     5,'F(+1/3)',8X,'FUNCTN',4X,'GRADNT',3X,'F(-1/3)',3X,'F(+1/3)')
 1004 FORMAT(10X,I4,1X,F10.2,1X,4F11.3,4X,4F10.4)
 1006 FORMAT(10X,I4,1X,F10.2,1X,2F11.3,26X,2F10.4)
 1008 FORMAT(/11X,'INFILTRATION RATE(CM/DAY)', 8(1H.),F8.3,17X,'MOISTURE
     1 ADDED TO PROFILE (CM3)', 6(1H.),F8.3,/11X,'DRAINAGE RATE(CM/DAY)'
     2,12(1H.),F8.3,17X,'MOISTURE INCREASE IN PROFILE(CM3)',4(1H.), F8.3
     3/11X,'TOTAL MOISTURE IN PROFILE(CM3)',3(1H.),F8.3,17X,'DEVIATION(C
     4M3)',23(1H.), F8.3)
      RETURN
      END
```

```
      FUNCTION SPR(MAT,N,PR)
C
C
C     PURPOSE: TO CALCULATE THE SOIL-HYDRAULIC PROPERTIES
C
      DIMENSION WCR(9), WCS(9), ALPHA(9), RN(9), CONDS(9), SS(9)
      DATA WCR/.200,.250,.170,.1611,.150,.140,.1311,.1244,.120/,WCS/.540
     1,.400,.470,.4611,.450,.440,.4311,.4244,.420/,ALPHA/.006,.009,.010,
     2.01036,.01080,.01120,.01156,.01182,.0120/,RN/1.60,3.0,2.0,2.178,2.
     340,2.60,2.778,2.911,3.00/,CONDS/25.,10.,75.,132.8,205.,270.,327.8,
     4371.1,400./,SS/4.E-07,5.E-08,1.E-07,1.E-07,1.E-07,1.E-07,1.E-07,
     51.E-07,1.E-07/
      DATA CONDM/1.E-08/
      IF(PR)1,10,10
    1 P=ABS(PR)
      A=ALPHA(MAT)
      R=RN(MAT)
      S=1.-1./R
      THETA=(1.+(A*P)**R)**(-S)
      IF(N-2) 2,4,6
    2 SPR=WCR(MAT)+(WCS(MAT)-WCR(MAT))*THETA
      RETURN
    4 T=1.-THETA*(A*P)**(R-1.)
      IF(THETA.LT.0.04) T=S*THETA**(1./S)
      COND=CONDS(MAT)*SQRT(THETA)*T*T
      SPR=AMAX1(COND,CONDM)
      RETURN
    6 T=1.+(A*P)**R
      WC=WCR(MAT)+(WCS(MAT)-WCR(MAT))*THETA
      SPR=(WC-WCR(MAT))*(R-1.)*A*(A*P)**(R-1.)/T + WC*SS(MAT)/WCS(MAT)
      RETURN
   10 GO TO (12,14,16,18),N
   12 SPR=WCS(MAT)
      RETURN
   14 SPR=CONDS(MAT)
      RETURN
   16 SPR=SS(MAT)
      RETURN
   18 THETA=(PR-WCR(MAT))/(WCS(MAT)-WCR(MAT))
      R=RN(MAT)
      S=R/(1.-R)
      IF(THETA.GT.0.999999) GO TO 20
      SPR=-(THETA**S-1.)**(1./R)/ALPHA(MAT)
      RETURN
   20 SPR=0.
      RETURN
      END
```